TABLE 3 The sequential differences in clinical isolates in *M. abscessus sensu lato*

Group	No. of tested strains	Predicted DDH result	Nucleotide sequence position[a]																												
			hsp65[b]							*rpoB*[c]																ITS region						
			115	118	127	187	190	229	340	10	31	79	88	124	127	136	193	202	277	283	316	343	376	379	25	45	48	60	101–103[d]	180	276
M. abscessus subsp. *abscessus*[T]	1	*M. abscessus*	T	T	C	C	C	G	C	T	T	C	T	G	C	T	C	C	C	C	C	T	C	C	C	T	A	C	A	C-G	C	G
Type 1	61	*M. abscessus*	T	T	C	C	C	G	C	T	T	C	T	G	C	T	C	C	C	C	C	T	C	C	C	T	A	C	A	C-G	C	G
Type 1a	6	*M. abscessus*	T	T	C	C	C	G	C	T	T	C	T	G	C	T	C	C	C	C	C	T	C	C	C	T	A	**T**	A	C-G	C	G
Type 1b	2	*M. abscessus*	T	T	C	C	C	G	**T**	T	T	C	T	G	C	T	C	C	C	C	T	C	C	C	T	A	**T**	A	C-G	C	G
M. abscessus subsp. *massiliense*[T]	1	*M. abscessus*	G	C	T	C	T	G	T	C	C	C	C	A	T	C	C	G	T	C	C	T	T	T	T	A	C	G	CCG	C	A
Type 2	29	*M. abscessus*	G	C	T	C	T	G	T	C	C	C	C	A	T	C	C	G	T	C	C	T	T	T	T	A	C	G	CCG	**T**	A
Type 2a	10	*M. abscessus*	G	C	T	C	T	G	T	C	C	C	C	A	T	C	C	G	T	C	C	T	T	**T**	**C**	A	C	G	CCG	**T**	A
Type 2b	2	*M. abscessus*	G	C	T	C	T	G	T	C	C	C	C	A	T	C	C	G	T	C	**T**	T	T	T	T	A	C	G	CCG	C	A
Type 2c	1	*M. abscessus*	G	C	T	C	T	G	T	C	C	C	C	A	T	C	C	G	T	C	**T**	T	T	T	**C**	A	C	G	CCG	C	A
Type 2d	1	*M. abscessus*	G	C	T	C	T	G	T	C	C	C	C	A	T	C	C	G	T	C	C	T	T	T	T	A	C	G	CCG	C	A
M. abscessus subsp. *bolletii*[T]	1	*M. abscessus*	G	C	T	T	T	C	C	G	T	T	C	A	T	C	T	T	T	T	T	T	T	T	T	A	C	A	C-G	C	G
Type 3a	1	*M. abscessus*	G	C	T	T	T	C	C	G	T	T	C	A	T	C	T	**C**	T	T	T	T	T	T	T	A	C	A	C-G	C	G
Type 3b	1	*M. abscessus*	G	C	T	T	T	C	C	G	T	T	C	A	T	C	T	**C**	T	T	T	T	T	T	T	**G**	C	A	C-G	C	G
Type 3c	1	*M. abscessus*	G	C	T	**C**	T	C	C	G	T	T	C	A	T	C	T	T	T	T	T	T	T	T	T	**G**	C	A	C-G	C	G
DS[e] type 4	2	*M. abscessus*	T	T	C	C	C	G	C	G	T	T	C	A	T	C	T	C	T	T	T	T	T	T	T	A	C	A	C-G	C	G
DS type 5	1	*M. abscessus*	G	C	T	C	T	G	T	T	T	C	T	G	C	T	C	C	C	C	T	C	C	C	T	A	C	G	CCG	C	A

[a] Bold letters indicate nucleotides different from those of the type strains.

[b] Nucleotide positions were based on the *M. abscessus* subsp. *massiliense* sequence of the partial *hsp65* gene (accession no. AB548601).

[c] Nucleotide positions were based on the *M. abscessus* subsp. *massiliense* sequence of the partial *rpoB* gene (accession no. AB548600).

[d] Base deficient.

[e] Isolate showing discordant sequencing results.

TABLE 4 Primers to discriminate reference strains of *M. abscessus* subsp. *abscessus* and *M. abscessus* subsp. *massiliense*

Primer	Sequence (locations)[a]	Amplified fragment size (ca. bp) of *M. abscessus* subsp. *abscessus*/*M. abscessus* subsp. *massiliense*[b]
MAB 0022cF	5′-TTCGATTCTCCTAGGCTCCA-3′ (22165–22184)	220/270
MAB 0022cR	5′-GGCGTACATGACCGCATACT-3′ (22386–22367)	
MAB 0104cF	5′-GGTGACTGAACTCCACGAAGA-3′ (105362–105382)	590/160
MAB 0104cR	5′-CGATATCGTGAGCCATCCTC-3′ (105948–105929)	
MAB 0357cF	5′-GGTAGCTCTTCCAGCCGAAT-3′ (354468–354487)	900/300
MAB 0357cR	5′-CAGCACGCA AAGGTACGAC-3′ (355376–355358)	
MAB 1112cF	5′-CCAAAACCGTTGAGCGTTAT-3′ (1125571–1125590)	200/1,020
MAB 1112cR	5′-ATCATGAACCGCAAGTACCG-3′ (1125776–1125757)	
MAB 1176cF	5′-CACACCACGTGTCCTACAGC-3′ (1193378–1193397)	210/860
MAB 1176cR	5′-AGTCCATCGAACGAACTTGG-3′ (1193594–1193575)	
MAB 2847cF	5′-CCCACAAATTTCGTAAGACCA-3′ (2896496–2896516)	130/200
MAB 2847cR	5′-ACCCAGGTGGAACTCTTCAC-3′ (2896628–2896609)	
MAB 3644F	5′-GTCACCGCAGAAATCGAGTC-3′ (3694129–3694148)	200/700
MAB 3644R	5′-GGGGTGGTTGACGTGTTC-3′ (3694310–3694293)	
MAB 3644 (Rev2R)[c]	5′-CGAGGTCAAGTGGCTTCTTT-3′ (3694262–3694243)	150/650
MAB 4614F	5′-CCTTCACCCTTCCGTTCAT-3′ (4698970–4698988)	215/535
MAB 4614R	5′-GTTGGGACTGCAGGTATTGC-3′ (4699184–4699165)	

[a] Nucleotide positions were based on the complete sequence of the *M. abscessus* subsp. *abscessus* chromosome (accession no. CU458896) as a reference.
[b] Fragment sizes were predicted from the results of sequencing of the draft genome of *M. abscessus* subsp. *massiliense* (accession no. BAOM01000001 to BAOM01000060).
[c] MAB 3644 (Rev2R) was used only in the multiplex PCR.

the proper size, although some of the clinical strains displayed contrasting results. We concluded that the combined targeting of MAB_0357c and MAB_3644 would produce the best results (Fig. 1 and 2). These regions generated amplicons of the correct size, delivered results that were consistent with those of multilocus sequence analysis, and provided an easy visual means to distinguish between *M. abscessus* subsp. *abscessus* and *M. abscessus* subsp. *massiliense*.

Discriminatory multiplex PCR assay. Based on the results of single PCR, we performed amplifications using the clinical strains. All of the clinical isolates that were initially identified as *M. abscessus* by DDH could be resolved as *M. abscessus* subsp. *abscessus* or *M. abscessus* subsp. *massiliense* using both sets of primer pairs MAB 0357c and MAB 3644. However, the amplification results were not always clear enough: it has been speculated that *Taq* polymerase is heavily utilized to amplify shorter bands, leaving many weak longer bands (data not shown). For more clearly balanced multiplex amplification, MAB 3644R was replaced with MAB 3644 (Rev2R) (Fig. 3). Using MAB 0357c and MAB 3644 (Rev2R) allowed a clear separation of *M. abscessus* subsp. *abscessus* isolates from *M. abscessus* subsp. *massiliense* isolates (Table 5; see also Table S1 in the supplemental material). Multiplex PCR results from the three type strains and 118 clinical isolates are shown in Table S1. A total of 70 *M. abscessus* subsp. *abscessus* isolates showed the same multiplex PCR pattern (ca. 900 bp and ca. 150 bp), and 44 *M. abscessus* subsp. *massiliense* isolates showed ca. 300 bp and ca. 650 bp. However, the results for 4 isolates of *M. abscessus* subsp. *bolletii* were not converged. One of the clinical isolates (type 3a) and the type strain showed an amplification pattern that was identical to that of *M. abscessus* subsp. *abscessus* (ca. 900 bp and ca. 150 bp). The two other clinical isolates (types 3b and 3c) showed different patterns, ca. 150 bp and ca. 300 bp and a weak pattern of ca. 300 bp and ca. 650 bp, respectively. The discordant results from two type 4 isolates were identical to those obtained for *M. abscessus* subsp. *bolletii* type 3b, showing a multiplex PCR pattern of ca. 150 bp and ca. 300 bp. The pattern determined for the remaining type 5 discordant isolate was identical to that of *M. abscessus* subsp. *massiliense*, ca. 300 bp and ca. 650 bp. All other mycobacterial isolates prepared as negative controls were negative in this multiplex PCR assay. The only exception was the *M. che-*

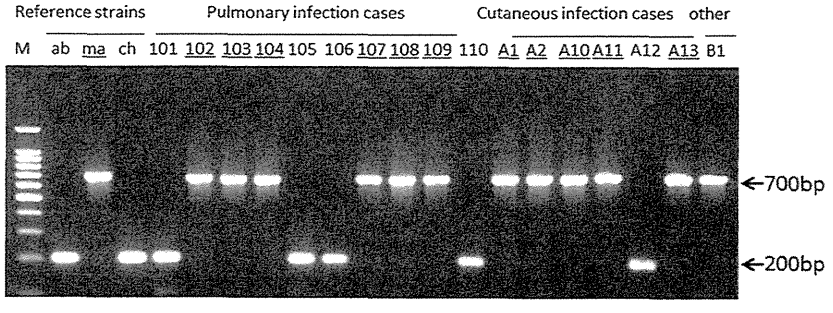

FIG 1 Representative single-PCR results for the reference strains and clinical isolates amplified with primer pair MAb 3644F and MAb 3644R. The numbers are the strain numbers of the clinical isolates. Underlining indicates that *M. abscessus* subsp. *massiliense* (ma) was classified after the multilocus genotyping assay shown in Table 3. The *M. abscessus* subsp. *massiliense* PCR product was fully amplified to 700 bp. However, the *M. abscessus* subsp. *abscessus* (ab) and *M. chelonae* (ch) amplicons amplified to 200 bp in size.

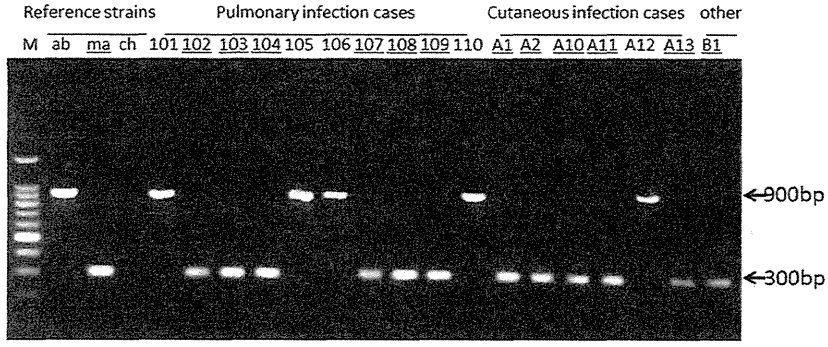

FIG 2 Representative single-PCR results for the reference strains and clinical isolates amplified with primer pair MAb 0357cF and MAb 0357cR. The numbers are the strain numbers of the clinical isolates. Underlining indicates that *M. abscessus* subsp. *massiliense* (ma) was classified after the multilocus genotyping assay shown in Table 3. The *M. abscessus* subsp. *abscessus* (ab) PCR product was fully amplified to 900 bp in size. However, the *M. abscessus* subsp. *massiliense* amplicon was 300 bp in size, while *M. chelonae* (ch) did not amplify.

lonae type strain, which showed a single weak band of ca. 200 bp (Fig. 3).

DISCUSSION

We have developed a simple, cost-effective discriminative multiplex PCR to differentiate *M. abscessus* subsp. *massiliense* from *M. abscessus* subsp. *abscessus* and from other RGM. The multiplex PCR expanded upon the results of two sets of discriminative single PCRs to concurrently amplify *M. abscessus* subsp. *abscessus* and *M. abscessus* subsp. *massiliense* and distinguish them based upon differences in amplicon size. In order to achieve the different amplifications in length, clear insertion or deletion regions between *M. abscessus* subsp. *massiliense* and *M. abscessus* subsp. *abscessus* whole-genome sequences were selected for the single-PCR targets using the Artemis Comparison Tool. The combination of MAB 0357c and MAB 3644 (Rev2R) for targeted PCR mainly leads to two distinct visual patterns that are easily read by novice PCR technologists. Previously, clinicians identified all isolates as *M. abscessus* because the use of the DDH assay was very common in Japan. The isolates were also grouped together because of their colony morphologies, growth profiles, and biochemical characteristics. Even the majority of the sequences of their 16S rRNA genes are the same. However, clinicians began to suspect that different strains were present because there were significantly different clinical outcomes and drug susceptibility groups among these isolates. For example, *M. abscessus* subsp. *massiliense* is more susceptible to azithromycin than *M. abscessus* subsp. *abscessus* but not to clofazimine, meropenem, and panipenem (17). Thus, correct and rapid species identification could facilitate the clinical treatment of mycobacterial infections (7). Two distinct genotypes were eventually observed in isolates identified as *M. abscessus* by the DDH mycobacterial assays (17). These two groups can be separated by a combinational genotypic analysis of the sequences of the ITS region and *hsp65* and *rpoB* genes. Similarly, in other reports of multilocus sequencing analysis performed with *hsp65*, *rpoB*, and *secA1* (4) or with eight housekeeping genes (29), *M. abscessus* subsp. *abscessus*, *M. abscessus* subsp. *massiliense*, and *M. abscessus* subsp. *bolletii* are clearly differentiated. But this methodology is not practical due to the cost and effort involved. There have been other PCR-based methods, such as erythromycin ribosome methyltransferase (*erm*) PCR (8) and variable-number tandem-repeat (VNTR) analysis (30). *erm* PCR is also a very simple and accurate method but, having only one target, can easily lead to false-negative results. The VNTR method is not easy for nonexperts.

A study in South Korea found that 51% of the *M. chelonae-M. abscessus* group is comprised of *M. abscessus* subsp. *abscessus* and 47% is *M. abscessus* subsp. *massiliense* (11). A typing study of *M. abscessus* subsp. *abscessus*, *M. abscessus* subsp. *massiliense*, and *M. abscessus* subsp. *bolletii* performed in the United States showed that 64% of the isolates were *M. abscessus* subsp. *abscessus* and 28% were *M. abscessus* subsp. *massiliense* (4). In France, 60% of the isolates belonged to *M. abscessus* subsp. *abscessus* and 22% to *M.*

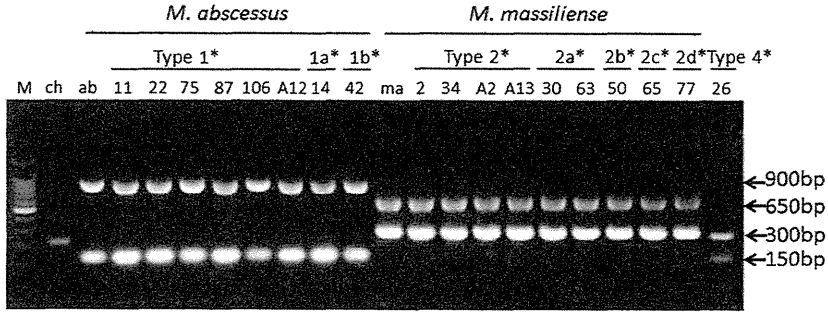

FIG 3 Representative multiplex PCR results for the reference strains and clinical isolates amplified with primer pair MAB 3644F and MAB 3644 (Rev2R) and primer pair MAB 0357cF and MAB 0357cR. *, types 1, 1a, and 1b, types 2, 2a, 2b, 2c, and 2d, and type 4 are the groupings of the clinical isolates based on their sequences (Table 3). The numerals below the groupings are the strain numbers of the clinical isolates.

TABLE 5 PCR results compared with other genetic classifications

Group	No. of tested strains	Predicted DDH result	Classification by *hsp65*/*rpoB*/ITS sequences[a]	PCR result(s) (ca. bp) with primer pair(s): MAB 3644F + MAB 3644R	MAB 0357cF + MAB 0357cR	MAB 3644F + MAB 3644 (Rev2R), MAB 0357cF + MAB 0357cR
M. abscessus subsp. *abscessus*^{T}	1	*M. abscessus*	*M. abscessus* subsp. *abscessus*	200	900	900, 150
Type 1	61	*M. abscessus*	*M. abscessus* subsp. *abscessus*	200	900	900, 150
Type 1a	6	*M. abscessus*	*M. abscessus* subsp. *abscessus*	200	900	900, 150
Type 1b	2	*M. abscessus*	*M. abscessus* subsp. *abscessus*	200	900	900, 150
M. abscessus subsp. *massiliense*^{T}	1	*M. abscessus*	*M. abscessus* subsp. *massiliense*	700	300	300, 650
Type 2	29	*M. abscessus*	*M. abscessus* subsp. *massiliense*	700	300	300, 650
Type 2a	10	*M. abscessus*	*M. abscessus* subsp. *massiliense*	700	300	300, 650
Type 2b	2	*M. abscessus*	*M. abscessus* subsp. *massiliense*	700	300	300, 650
Type 2c	1	*M. abscessus*	*M. abscessus* subsp. *massiliense*	700	300	300, 650
Type 2d	1	*M. abscessus*	*M. abscessus* subsp. *massiliense*	700	300	300, 650
M. abscessus subsp. *bolletii*^{T}	1	*M. abscessus*	*M. abscessus* subsp. *bolletii*	200	900	900, 150
Type 3a	1	*M. abscessus*	*M. abscessus* subsp. *bolletii*	200	900	900, 150
Type 3b	1	*M. abscessus*	*M. abscessus* subsp. *bolletii*	200	300	300, 150
Type 3c	1	*M. abscessus*	*M. abscessus* subsp. *bolletii*	700	300[b]	300[b], 650
DS[c] type 4	2	*M. abscessus*	*M. abscessus* subsp. *abscessus*-*M. abscessus* subsp. *bolletii*[d]	200	300	300, 150
DS type 5	1	*M. abscessus*	*M. abscessus* subsp. *massiliense*-*M. abscessus* subsp. *abscessus*[e]	700	300	300, 650

[a] Classifications were determined on the basis of the overall results of sequencing of *hsp65*, *rpoB*, and the ITS region (Table 3).
[b] Weak band.
[c] Isolate showing discordant sequencing results.
[d] Isolate showing *M. abscessus* subsp. *abscessus hsp65* and *M. abscessus* subsp. *bolletii rpoB* sequences.
[e] Isolate showing *M. abscessus* subsp. *massiliense hsp65* and ITS region and *M. abscessus* subsp. *abscessus rpoB* sequences.

abscessus subsp. *massiliense* (13), while in Japan, 71% belonged to *M. abscessus* subsp. *abscessus* and 26% to *M. abscessus* subsp. *massiliense* (20). In pulmonary patients in the Netherlands diagnosed with infections by strains from the *M. chelonae-M. abscessus* group, 50% of the isolates were identified as *M. abscessus* subsp. *abscessus* and 29% as *M. abscessus* subsp. *massiliense* (31). In accordance with the recent study in Japan mentioned above (20), we can estimate that more than 30% of patients diagnosed with *M. abscessus* subsp. *abscessus* should differentiate as *M. abscessus* subsp. *massiliense* patients. Some isolates might be colonizers whereas others might have appeared after prolonged treatment of infections by other nontuberculous mycobacteria. Therefore, we are currently collecting patient treatment data from the hospitals that participated in this study and are analyzing the relationship between clinical isolates and treatment history.

Three clinical isolates were not identified to the species level by multilocus sequence analysis. They are discordant isolates that were previously reported by Zelazny et al. (4) and Macheras et al. (29). The sequences of the *hsp65* genes and ITS regions of the two isolates were identical to those of *M. abscessus* subsp. *abscessus*; however, they carried the *rpoB* sequence of *M. abscessus* subsp. *bolletii* with the 1-bp mismatch (DS type 4). Both strains produced multiplex PCR amplicons of ca. 300 bp and ca. 150 bp, like those of *M. abscessus* subsp. *bolletii* type 3b (see Table S1 in the supplemental material). The third isolate which had the *M. abscessus* subsp. *massiliense hsp65* and ITS regions and the *rpoB* sequence of *M. abscessus* subsp. *abscessus* (DS type 5) had the multiplex PCR pattern of *M. abscessus* subsp. *massiliense* (ca. 300 bp and ca. 650 bp). Although those strains are very rare, they are interesting in that they suggest the occurrence of horizontal gene transfer. Such discordant isolates would produce different amplicons (ca. 300 bp and ca. 150 bp) from *M. abscessus* subsp. *abscessus* and *M. abscessus* subsp. *massiliense* (Table 5).

In the case of RGM infection, we propose the use of this multiplex PCR assay as a first step, because it can be used by inexperienced technicians to identify *M. abscessus* subsp. *abscessus* and *M. abscessus* subsp. *massiliense* quickly and accurately. In addition, there is no need to prepare purified DNA; the supernatant from a boiled bacterial suspension can be used (data not shown). The resulting band patterns of 900 bp and 150 bp and of 300 bp and 650 bp imply the identification of *M. abscessus* subsp. *abscessus* and *M. abscessus* subsp. *massiliense* with 97.2% and 95.7% accuracy. Another rare pattern, 300 bp and 150 bp, implies identification of a discordant strain with 66.7% accuracy. Although this multiplex PCR method conduces to reasonably accurate discrimination, it cannot be used to differentiate *M. abscessus* subsp. *bolletii* from *M. abscessus* subsp. *abscessus* or *M. abscessus* subsp. *massiliense*, because all three clinical isolates of *M. abscessus* subsp. *bolletii* showed different multiplex PCR patterns in this study (Table 5).

As a result of this study, we have developed a simple, rapid

methodology to distinguish between *M. abscessus* subsp. *abscessus* and *M. abscessus* subsp. *massiliense*. This approach, which spans whole-genome sequencing and clinical diagnosis, will facilitate the acquisition of more precise information about bacterial genomes, aid in the choice of more-relevant therapies, and promote the advancement of novel discrimination and differential diagnostic assays.

APPENDIX

The clinical isolates used in this study were sent from the hospitals and universities described below. Specimens were originally collected for disease diagnosis. The portion remaining after diagnosis was used for this study. We appreciate the work of all of the clinicians in the following institutions who took care of patients infected with these mycobacteria: Hokkaido Social Insurance Hospital, Japan Anti-Tuberculosis Association (JATA) Fukujuji Hospital, Saitama Medical University, National Hospital Organization (NHO) Tokyo National Hospital, Showa University Fujigaoka Hospital, National Defense Medical College Hospital, Kyorin University Hospital, NHO Minami-Kyoto Hospital, Kyoto Prefectural University of Medicine, JATA Osaka Hospital, NHO Kinki-Chuo Chest Medical Center, NHO Matsue Medical Center, NHO Higashihiroshima Medical Center, Kawasaki Medical School, Kyosai-Yoshijima Hospital, and NHO Omuta Hospital.

ACKNOWLEDGMENTS

We appreciate Ms Katsue Ishii (Fukujuji Hospital) for preparing negative control of clinical isolates.

This work was supported in part by a Grant-in-Aid for Research on Emerging and Re-emerging Infectious Diseases from the Ministry of Health, Labor, and Welfare of Japan for Y.H., M.M., and N.I. and by a Grant-in-Aid for Scientific Research (C) from the Ministry of Education, Culture, Sports, Science and Technology of Japan for Y.H. and by a Grant-in-Aid for Scientific Research (C) from the Japan Society for the Promotion of Science for K.N.

REFERENCES

1. **Viana-Niero C, Lima KV, Lopes ML, Rabello MC, Marsola LR, Brilhante VC, Durham AM, Leão SC.** 2008. Molecular characterization of *Mycobacterium massiliense* and *Mycobacterium bolletii* in isolates collected from outbreaks of infections after laparoscopic surgeries and cosmetic procedures. J. Clin. Microbiol. **46**:850–855. http://dx.doi.org/10.1128/JCM.02052-07.
2. **Simmon KE, Pounder JI, Greene JN, Walsh F, Anderson CM, Cohen S, Petti CA.** 2007. Identification of an emerging pathogen, Mycobacterium massiliense, by *rpoB* sequencing of clinical isolates collected in the United States. J. Clin. Microbiol. **45**:1978–1980. http://dx.doi.org/10.1128/JCM.00563-07.
3. **Cardoso AM, Martins de Sousa E, Viana-Niero C, Bonfim de Bortoli F, Pereira das Neves ZC, Leão SC, Junqueira-Kipnis AP, Kipnis A.** 2008. Emergence of nosocomial *Mycobacterium massiliense* infection in Goiás, Brazil. Microbes Infect. **10**:1552–1557. http://dx.doi.org/10.1016/j.micinf.2008.09.008.
4. **Zelazny AM, Root JM, Shea YR, Colombo RE, Shamputa IC, Stock F, Conlan S, McNulty S, Brown-Elliott BA, Wallace RJ, Jr, Olivier KN, Holland SM, Sampaio EP.** 2009. Cohort study of molecular identification and typing of *Mycobacteriumabscessus*,*Mycobacterium massiliense*, and *Mycobacterium bolletii*. J. Clin. Microbiol. **47**:1985–1995. http://dx.doi.org/10.1128/JCM.01688-08.
5. **Adékambi T, Reynaud-Gaubert M, Greub G, Gevaudan MJ, La Scola B, Raoult D, Drancourt M.** 2004. Amoebal coculture of "*Mycobacterium massiliense*" sp. nov. from the sputum of a patient with hemoptoic pneumonia. J. Clin. Microbiol. **42**:5493–5501. http://dx.doi.org/10.1128/JCM.42.12.5493-5501.2004.
6. **Adékambi T, Berger P, Raoult D, Drancourt M.** 2006. rpoB gene sequence-based characterization of emerging non-tuberculous mycobacteria with descriptions of *Mycobacterium bolletii sp. nov.*, *Mycobacterium phocaicum* sp. nov. and *Mycobacterium aubagnense* sp. nov. Int. J. Syst. Evol. Microbiol. **56**(Pt 1):133–143. http://dx.doi.org/10.1099/ijs.0.63969-0.
7. **Koh WJ, Jeon K, Lee NY, Kim BJ, Kook YH, Lee SH, Park YK, Kim CK, Shin SJ, Huitt GA, Daley CL, Kwon OJ.** 2011. Clinical significance of differentiation of *Mycobacterium massiliense* from *Mycobacterium abscessus*. Am. J. Respir. Crit. Care Med. **183**:405–410. http://dx.doi.org/10.1164/rccm.201003-0395OC.
8. **Kim HY, Kim BJ, Kook Y, Yun YJ, Shin JH, Kim BJ, Kook YH.** 2010. *Mycobacterium massiliense* is differentiated from *Mycobacterium abscessus* and *Mycobacterium bolletii* by erythromycin ribosome methyltransferase gene (erm) and clarithromycin susceptibility patterns. Microbiol. Immunol. **54**:347–353. http://dx.doi.org/10.1111/j.1348-0421.2010.00221.x.
9. **Leao SC, Tortoli E, Euzéby JP, Garcia MJ.** 2011. Proposal that *Mycobacterium massiliense* and *Mycobacterium bolletii* be united and reclassified as *Mycobacterium abscessus* subsp. *bolletii* comb. nov., designation of *Mycobacterium abscessus* subsp. *abscessus* subsp. nov. and emended description of *Mycobacterium abscessus*. Int. J. Syst. Evol. Microbiol. **61**(Pt 9):2311–2313. http://dx.doi.org/10.1099/ijs.0.023770-0.
10. **Bryant JM, Grogono DM, Greaves D, Foweraker J, Roddick I, Inns T, Reacher M, Haworth CS, Curran MD, Harris SR, Peacock SJ, Parkhill J, Floto RA.** 2013. Whole-genome sequencing to identify transmission of *Mycobacterium abscessus* between patients with cystic fibrosis: a retrospective cohort study. Lancet **381**:1551–1560. http://dx.doi.org/10.1016/S0140-6736(13)60632-7.
11. **Kim HY, Yun YJ, Park CG, Lee DH, Cho YK, Park BJ, Joo SI, Kim EC, Hur YJ, Kim BJ, Kook YH.** 2007. Outbreak of *Mycobacterium massiliense* infection associated with intramuscular injections. J. Clin. Microbiol. **45**:3127–3130. http://dx.doi.org/10.1128/JCM.00608-07.
12. **Tortoli E, Gabini R, Galanti I, Mariottini A.** 2008. Lethal *Mycobacterium massiliense* sepsis, Italy. Emerg. Infect. Dis. **14**:984–985. http://dx.doi.org/10.3201/eid1406.080194.
13. **Roux AL, Catherinot E, Ripoll F, Soismier N, Macheras E, Ravilly S, Bellis G, Vibet MA, Le Roux E, Lemonnier L, Gutierrez C, Vincent V, Fauroux B, Rottman M, Guillemot D, Gaillard JL; Jean-Louis Herrmann for the Group OMA.** 2009. Multicenter study of prevalence of nontuberculous mycobacteria in patients with cystic fibrosis in France. J. Clin. Microbiol. **47**:4124–4128. http://dx.doi.org/10.1128/JCM.01257-09.
14. **Kobashi Y, Mouri K, Obase Y, Miyashita N, Nakanaga K, Oka M.** 2011. Pulmonary *Mycobacterium massiliense* disease with septicemia during immunosuppressive treatment. Intern. Med. **50**:1069–1073. http://dx.doi.org/10.2169/internalmedicine.50.4733.
15. **Hamamoto T, Yuki A, Naoi K, Kawakami S, Banba Y, Yamamura T, Hikota R, Watanabe J, Kimura F, Nakanaga K, Hoshino Y, Ishii N, Shimazaki H, Nakanishi K, Tamai S.** 2012. Bacteremia due to *Mycobacterium massilinese* in a patient with chronic myelogenous leukemia: case report. Diagn. Microbiol. Infect. Dis. **74**:183–185. http://dx.doi.org/10.1016/j.diagmicrobio.2012.06.009.
16. **Otsuki T, Izaki S, Nakanaga K, Hoshino Y, Ishii N, Osamura K.** 2012. Cutaneous *Mycobacterium massiliense* infection: a sporadic case in Japan. J. Dermatol. **39**:569–572. http://dx.doi.org/10.1111/j.1346-8138.2011.01339.x.
17. **Nakanaga K, Hoshino Y, Era Y, Matsumoto K, Kanazawa Y, Tomita A, Furuta M, Washizu M, Makino M, Ishii N.** 2011. Multiple cases of cutaneous *Mycobacterium massiliense* infection in a "hot spa" in Japan. J. Clin. Microbiol. **49**:613–617. http://dx.doi.org/10.1128/JCM.00817-10.
18. **Choi GE, Shin SJ, Won CJ, Min KN, Oh T, Hahn MY, Lee K, Lee SH, Daley CL, Kim S, Jeong BH, Jeon K, Koh WJ.** 2012. Macrolide treatment for *Mycobacterium abscessus* and *Mycobacterium massiliense* infection and inducible resistance. Am. J. Respir. Crit. Care Med. **186**:917–925. http://dx.doi.org/10.1164/rccm.201111-2005OC.
19. **Kusunoki S, Ezaki T, Tamesada M, Hatanaka Y, Asano K, Hashimoto Y, Yabuuchi E.** 1991. Application of colorimetric microdilution plate hybridization for rapid genetic identification of 22 *Mycobacterium* species. J. Clin. Microbiol. **29**:1596–1603.
20. **Harada T, Akiyama Y, Kurashima A, Nagai H, Tsuyuguchi K, Fujii T, Yano S, Shigeto E, Kuraoka T, Kajiki A, Kobashi Y, Kokubu F, Sato A, Yoshida S, Iwamoto T, Saito H.** 2012. Clinical and microbiological differences between *Mycobacterium abscessus* and *Mycobacterium massiliense* lung diseases. J. Clin. Microbiol. **50**:3556–3561. http://dx.doi.org/10.1128/JCM.01175-12.
21. **Springer B, Wu WK, Bodmer T, Haase G, Pfyffer GE, Kroppenstedt RM, Schroder KH, Emler S, Kilburn JO, Kirschner P, Telenti A, Coyle MB, Böttger EC.** 1996. Isolation and characterization of a unique group of slowly growing mycobacteria: description of *Mycobacterium lentiflavum* sp. nov. J. Clin. Microbiol. **34**:1100–1107.

22. **Telenti A, Marchesi F, Balz M, Bally F, Böttger EC, Bodmer T.** 1993. Rapid identification of mycobacteria to the species level by polymerase chain reaction and restriction enzyme analysis. J. Clin. Microbiol. **31**:175–178.
23. **Roth A, Fischer M, Hamid ME, Michalke S, Ludwig W, Mauch H.** 1998. Differentiation of phylogenetically related slowly growing mycobacteria based on 16S-23S rRNA gene internal transcribed spacer sequences. J. Clin. Microbiol. **36**:139–147.
24. **Nakanaga K, Ishii N, Suzuki K, Tanigawa K, Goto M, Okabe T, Imada H, Kodama A, Iwamoto T, Takahashi H, Saito H.** 2007. "*Mycobacterium ulcerans* subsp. *shinshuense*" isolated from a skin ulcer lesion: identification based on 16S rRNA gene sequencing. J. Clin. Microbiol. **45**:3840–3843. http://dx.doi.org/10.1128/JCM.01041-07.
25. **Chaisson MJ, Pevzner PA.** 2008. Short read fragment assembly of bacterial genomes. Genome Res. **18**:324–330. http://dx.doi.org/10.1101/gr.7088808.
26. **Richter DC, Schuster SC, Huson DH.** 2007. OSLay: optimal syntenic layout of unfinished assemblies. Bioinformatics **23**:1573–1579. http://dx.doi.org/10.1093/bioinformatics/btm153.
27. **Altschul SF, Madden TL, Schaffer AA, Zhang J, Zhang Z, Miller W, Lipman DJ.** 1997. Gapped BLAST and PSI-BLAST: a new generation of protein database search programs. Nucleic Acids Res. **25**:3389–3402. http://dx.doi.org/10.1093/nar/25.17.3389.
28. **Carver TJ, Rutherford KM, Berriman M, Rajandream MA, Barrell BG, Parkhill J.** 2005. ACT: the Artemis Comparison Tool. Bioinformatics **21**:3422–3423. http://dx.doi.org/10.1093/bioinformatics/bti553.
29. **Macheras E, Roux AL, Ripoll F, Sivadon-Tardy V, Gutierrez C, Gaillard JL, Heym B.** 2009. Inaccuracy of single-target sequencing for discriminating species of the *Mycobacterium abscessus* group. J. Clin. Microbiol. **47**:2596–2600. http://dx.doi.org/10.1128/JCM.00037-09.
30. **Wong YL, Ong CS, Ngeow YF.** 2012. Molecular typing of *Mycobacterium abscessus* based on tandem-repeat polymorphism. J. Clin. Microbiol. **50**:3084–3088. http://dx.doi.org/10.1128/JCM.00753-12.
31. **van Ingen J, de Zwaan R, Dekhuijzen RP, Boeree MJ, van Soolingen D.** 2009. Clinical relevance of *Mycobacterium chelonae-abscessus* group isolation in 95 patients. J. Infect. **59**:324–331. http://dx.doi.org/10.1016/j.jinf.2009.08.016.

Pathogens and Disease ISSN 2049-632X

RESEARCH ARTICLE

The RD1 locus in the *Mycobacterium tuberculosis* genome contributes to the maturation and secretion of IL-1α from infected macrophages through the elevation of cytoplasmic calcium levels and calpain activation

Ruili Yang[1,2], Chen Xi[2,3], Dewamitta R. Sita[2], Shunsuke Sakai[2], Kohsuke Tsuchiya[2], Hideki Hara[2], Yanna Shen[2], Huixin Qu[2], Rendong Fang[2], Masao Mitsuyama[2] & Ikuo Kawamura[2]

1 Department of Pathogenic Biology and Immunology, School of Medicine, Southeast University, Nanjing, China
2 Department of Microbiology, Kyoto University Graduate School of Medicine, Sakyo-ku, Kyoto, Japan
3 Department of Molecular and Biology, Beijing Tuberculosis and Thoracic Tumor Research Institute, Beijing, China

This is a well-written and detailed report proceeds logically with a series of *in vitro* experiments that show that release of mature IL-1alpha by macrophages following a *Mycobacterium tuberculosis* infection is dependent on RD1. The requirements for the cysteine protease calpain and for RD1-dependent increase of intracellular Ca^{2+} levels for cleavage of pro-IL-1alpha are demonstrated.

Keywords
Mycobacterium tuberculosis; RD1; macrophage; IL-1α; calpain; calcium.

Correspondence
Ikuo Kawamura, Department of Microbiology, Kyoto University, Graduate School of Medicine, Yoshidakonoe-cho, Sakyo-ku, Kyoto 606-8501, Japan.
Tel.: +81 75 753 4447
fax: +81 75 753 4446
e-mail: ikuo_kawamura@mb.med.kyoto-u.ac.jp

Received 16 April 2013; revised 30 June 2013; accepted 23 July 2013. Final version published online 23 August 2013.

doi:10.1111/2049-632X.12075

Editor: Patricia Bozza

Abstract

Region of difference 1 (RD1) is a genomic locus in the *Mycobacterium tuberculosis* genome that has been shown to participate in the virulence of the bacterium, induction of cell death, and cytokine secretion in infected macrophages. In this study, we investigated the role of RD1 in interleukin-1α (IL-1α) secretion. *M. tuberculosis* H37Rv strain, but not a mutant strain deficient for RD1 (ΔRD1), significantly induced IL-1α secretion from infected macrophages. Although IL-1α secretion was only observed in H37Rv-infected macrophages, there was no difference in the level of IL-1α transcription and pro-IL1α synthesis after infection with H37Rv and ΔRD1. Interestingly, ΔRD1 infection did not increase intracellular Ca^{2+} levels, and Ca^{2+} chelators markedly inhibited IL-1α secretion in response to H37Rv infection. Moreover, the inability of ΔRD1 to induce IL-1α secretion was restored by treatment with the calcium ionophore A23187. A significant increase in calpain activity was detected in macrophages infected with H37Rv, but not with ΔRD1, and calpain inhibitors abrogated IL-1α secretion. Taken together, these results suggest that in *M. tuberculosis*-infected macrophages, RD1 contributed to maturation and secretion of IL-1α by enhancing the influx of Ca^{2+} followed by calpain activation.

Introduction

Mycobacterium tuberculosis, an etiologic agent of tuberculosis, is one of the leading threats to humans. Based on estimates by the World Health Organization (WHO), *M. tuberculosis* caused 8.7 million new cases of tuberculosis and 1.4 million deaths worldwide in 2011 (WHO, 2012). The recent emergence of extensively drug-resistant *M. tuberculosis* and its co-infection with HIV highlights the urgent need for an improved understanding of the pathogenesis of *M. tuberculosis*, which may identify novel approaches to treat and prevent tuberculosis (O'Donnell *et al.*, 2013).

A genomic locus of *M. tuberculosis* called 'region of difference 1' (RD1) is approximately 9.5 kb in length, and it was first discovered as a region that is absent in a genome of *M. bovis* BCG (Mahairas *et al.*, 1996). RD1 is critical for bacterial virulence (Pym *et al.*, 2002; Stanley *et al.*, 2003, 2007; Gao *et al.*, 2004; Guinn *et al.*, 2004; Majlessi *et al.*, 2005; Brodin *et al.*, 2006), necrosis induction (Hsu *et al.*, 2003; Junqueira-Kipnis *et al.*, 2006; Chen *et al.*, 2007; Kaku *et al.*, 2007), granuloma formation (Volkman *et al.*, 2004), and the generation of protective immunity (Pym *et al.*, 2003; Brodin *et al.*, 2004a). RD1 is located in the ESX-1 locus (Feltcher *et al.*, 2011), which is one of the specialized export systems of *M. tuberculosis*. The ESX-1 system is named for

the secretory component, the 6-kDa early secreted antigenic target (ESAT-6) of *M. tuberculosis* and has been referred to as a type VII secretion system (Abdallah *et al.*, 2007). The ESX-1 locus contains genes encoding secretory proteins and a suite of genes encoding the secretion machinery (Feltcher *et al.*, 2011). Although all the components have not yet been fully characterized, proteins with known functional domains were identified. They include putative chaperones with an AAA^+ ATPase (Rv3868; EccA1, Rv3871; EccCb1), a subtilisin-like serine protease (Rv3883c; MycP1), and FtsK/SpoIIIE-like ATPase (Rv3870; EccCa1). EccB1 and EccE1 are shown to serve as core components of ESX-1. *rv3877* (*eccD1*) is located in the RD1 region and predicted to be a membrane-spanning protein that could be part of the translocation pore in the cytoplasmic membrane. The RD1 region also contains genes coding for two secretory components, ESAT-6 (EsxA) and culture filtrate protein of 10 kDa (CFP-10; EsxB). Therefore, deletion of the RD1 locus completely abrogates the ESX-1 secretory system.

Upon infection with *M. tuberculosis*, macrophages secrete a variety of cytokines, including tumor necrosis factor-alpha (TNF-α), interleukin-1α (IL-1α), IL-1β, IL-6, IL-12, and IL-18 (Patel *et al.*, 2007; Kurenuma *et al.*, 2009). *Mycobacterium tuberculosis* infection is accompanied by an intense local inflammation, which is likely due to these proinflammatory cytokines. In fact, TNF-α, IL-1, and IL-6 mediate the tissue injury in animal models of tuberculosis (Grover *et al.*, 2008). IL-1 is a prototypic multifunctional cytokine and was initially characterized as a factor that causes fever and augments lymphocyte responses (Dinarello, 1996). In addition, several studies have shown that IL-1α is recognized as a danger signal that is released from necrotic cells and functions as a key mediator of the inflammatory response (Chen *et al.*, 2007; Sims & Smith, 2010). Furthermore, IL-1α secretion could be of significance in terms of spreading proinflammatory signals to healthy neighboring cells *in vivo* (Schaub *et al.*, 2003), suggesting that IL-1α plays a key role in the pathological outcome. On the other hand, recent reports have shown that IL-1 receptor knockout mice are highly susceptible to *M. tuberculosis* infection (Fremond *et al.*, 2007), and both IL-1α and IL-1β serve as mediators of protective immune responses to *M. tuberculosis* (Mayer-Barber *et al.*, 2001; Guler *et al.*, 2011). These findings suggest that IL-1α, together with IL-1β, is critical to controlling acute *M. tuberculosis* infection and that coordinated regulation of IL-1 activity may be necessary to govern host immune response to *M. tuberculosis*.

Mycobacterium tuberculosis infection induces the production of the proinflammatory cytokines IL-1α, IL-1β, and IL-18, which belong to the IL-1 superfamily (Sims & Smith, 2010). IL-1β and IL-18 are produced as proforms that are cleaved by caspase-1 and secreted as an active form. Previous studies demonstrated the activation of caspase-1 by the induction of potassium ion efflux in *M. tuberculosis*-infected macrophages, and the RD1 locus of *M. tuberculosis* was required for the induction this ion efflux (Kurenuma *et al.*, 2009). In addition to IL-1β, a large amount of IL-1α is produced by infected macrophages, and calpain, a Ca^{2+}-dependent cysteine protease, is predicted to contribute to the processing and secretion of IL-1α (Carruth *et al.*, 1991; Goll *et al.*, 2003). However, the precise mechanism underlying IL-1α secretion remains undefined. In this study, we determined that *M. tuberculosis* infection induced IL-1α mRNA expression and pro-IL1α synthesis independently of RD1. Furthermore, the RD1 gene locus was indispensable for the induction of Ca^{2+} influx and the activation of calpain, which were required for the processing and secretion of IL-1α.

Materials and methods

Reagents

EGTA was purchased from Nacalai Tesque Inc. (Kyoto, Japan). BAPTA-AM and A23187 were obtained from Sigma-Aldrich (St. Louis, MO). Calpain inhibitors, MDL28170 (carbobenzoxy-valyl-phenylalanial), EST ((2*S*,3*S*)-*trans*-epoxysuccinyl-L-leucylamido-3-methylbutane ethyl ester), and calpain inhibitor IV (Z-LLY-FMK), were obtained from Merck Chemicals (Tokyo, Japan).

Mice

Female C57BL/6 mice were purchased from Japan SLC (Hamamatsu, Japan). Mice were maintained under specific pathogen-free conditions and used at 7–9 weeks of age. All animal experiments were approved by the Animal Ethics and Research Committee of Kyoto University Graduate School of Medicine.

Bacteria

The following *M. tuberculosis* strains were kindly provided by Prof. William R. Jacobs (Albert Einstein Institute, Bronx, NY) (Hsu *et al.*, 2003): H37Rv strain, an H37Rv mutant strain deficient for the RD1 locus (ΔRD1), and an RD1-complemented strain (ΔRD1::RD1). These *M. tuberculosis* strains were grown at 37 °C to mid-log phase in Middlebrook 7H9 broth supplemented with 0.5% albumin, 0.2% dextrose, 3 μg mL^{-1} catalase, and 0.2% glycerol. Bacteria were harvested, stirred vigorously with glass beads (3 mm in diameter), and centrifuged at 300 × ***g*** for 3 min to remove the bacterial clumps. The suspension was stored at −80 °C in aliquots. After thawing, the number of viable bacteria was enumerated by counting the colonies after plating the diluted suspension on Middlebrook 7H10 agar plates containing enrichments (50 μg mL^{-1} oleic acid, 0.5% albumin, 0.2% dextrose, 4 μg mL^{-1} catalase, and 0.85 mg mL^{-1} sodium chloride).

Macrophages

Peritoneal exudate cells were obtained by a peritoneal lavage 4 days after an intraperitoneal injection with 3 mL of thioglycollate medium (EIKEN Chemical, Osaka, Japan) and plated at 5.0×10^5 cells $well^{-1}$ in 48-well tissue culture plates. After incubation for 3 h, nonadherent cells were removed and adherent cells were used as macrophages. Based on Giemsa staining and a phagocytosis assay using

latex beads, more than 98% of adherent cells were identified as macrophages.

Intracellular growth of bacteria

Macrophages were infected with H37Rv, ΔRD1, and ΔRD1::RD1 at a multiplicity of infection (MOI) of 5 for 3 h. Cells were washed to remove extracellular bacteria and cultured for 21 h at 37 °C. Cells were then lysed in phosphate-buffered saline (PBS) containing 0.05% Triton X-100, and the number of viable bacteria was enumerated by inoculating the cell lysate on Middlebrook 7H10 agar plates containing enrichments and counting colonies 3 weeks later.

Real-time RT-PCR

Macrophages were infected with H37Rv, ΔRD1, and ΔRD1::RD1 at a MOI of 5 for 3 h, washed, and cultured for 3 h. Total RNA was extracted using the Nucleospin RNA II kit (Macherey-Nagel, Duren, Germany). Total RNA (0.2 μg) was treated with an RNase-free DNase (Promega, Tokyo, Japan) and subjected to reverse transcription (RT) using a Super-Script III first-strand synthesis system for RT-PCR (Invitrogen, Tokyo, Japan). Quantitative real-time RT-PCR was performed on an ABI Prism 7000 (Applied Biosystems, Foster City, CA) using a Platinum SYBR green qPCR SuperMix-UDG (Invitrogen) according to the manufacturer's instructions. The level of IL-1α mRNA was normalized on the basis of β-actin mRNA expression and analyzed with ABI Prism 7000 SDS software. DNA sequences of the PCR primers are as follows: IL-1α, 5′-CTCTAGAGCACCATGCTACAGAC-3′ (forward) and 5′-TGGAATCCAGGGGAAACACTG-3′ (reverse); and β-actin, 5′-TGGAATCCTGTGGCATCCATGAAAC-3′ (forward) and 5′-TAAAACGCAGCTCAGTAACAGTCCG-3′ (reverse).

Cytokine assay

Macrophages were infected with H37Rv, ΔRD1, and ΔRD1::RD1 at a MOI of 5 for 3 h. Cells were washed to remove extracellular bacteria and cultured for 21 h. The culture supernatant was collected, and the levels of IL-1α and IL-12/23p40 were determined by the OptEIA mouse IL-1α ELISA set and the OptEIA mouse IL-12/23p40 ELISA set (BD Bioscience Pharmingen, San Diego, CA), respectively. In one experiment, macrophages were infected with each of three *M. tuberculosis* strains for 3 h, washed, and cultured for 3, 6, 9, 12, and 21 h. The culture supernatant was collected, and the level of IL-1α was measured. Concomitantly, cells were lysed in PBS containing 1% Triton X-100 at each time point. The lysate was centrifuged to prepare the cleared cell lysate, and the level of IL-1α in the cell lysate was also measured. Alternatively, macrophages were infected with ΔRD1 at a MOI of 5 for 3 h. Cells were washed and incubated for 21 h in the presence or absence of 10 μM A23187. The culture supernatant was collected, and IL-1α concentration was determined. In addition, macrophages were infected with *M. tuberculosis* strains and cultured as described above. The culture supernatant was collected, and cells were lysed in 10 mM HEPES buffer (pH 7.5) containing 150 mM NaCl, 1% Nonidet P-40, 10% glycerol, 1 mM EDTA, and a protease/phosphatase inhibitor cocktail (Nacalai Tesque Inc., Kyoto, Japan). The culture supernatant and the cell lysate were subjected to SDS-PAGE, and separated proteins were transferred to a polyvinylidene difluoride membrane by electroblotting. To detect pro-IL1α (35 kDa) and mature IL-1α (17 kDa), the membrane was treated sequentially with biotinylated goat anti-IL-1α polyclonal antibody (Genzyme, Cambridge, MA) and streptavidin–horseradish peroxidase (HRP) conjugate (Invitrogen). After a brief incubation of the membrane in ECL Plus (GE Healthcare Bio-Sciences AB, Uppsala, Sweden), the bands representative of pro-IL-1α and mature IL-1α were detected in a LAS-4000 mini imager (Fuji Film, Tokyo, Japan).

Calpain activation

Macrophages were infected with H37Rv for 3 h. Cells were washed to remove extracellular bacteria, cultured for 3 h, and then treated for 21 h with or without 1 mM EGTA, 20 μM BAPTA-AM, 10–40 μM MDL28170, 100 μM calpain inhibitor IV, and 100 μM EST. The culture supernatant was collected, and the level of IL-1α was measured by ELISA or Western blotting. Preliminary studies showed that the concentration ranges of the Ca^{2+} chelators and calpain inhibitors exhibited no direct cytotoxicity to macrophages (data not shown). In one experiment, macrophages were infected with three *M. tuberculosis* strains for 3 h, washed, and cultured for 3, 6, 9, 12, and 24 h. The culture supernatants were collected, and the cell lysates were prepared for each culture period. To evaluate calpain activity, the culture supernatants and the cell lysates were subjected to SDS-PAGE and Western blotting using anti-α-fodrin monoclonal antibody (Chemicon International, Temecula, CA) and HRP-conjugated anti-mouse IgG1 antibody (Invitrogen). We monitored the amount of the proteolytic fragment of α-fodrin, an internal substrate of calpain, in the culture supernatant and that of full-length α-fodrin in the cell lysate.

Lactate dehydorogenase (LDH) release

Macrophages were infected with H37Rv, ΔRD1, and ΔRD1::RD1 for 3 h, washed, and then cultured for 21 h. The LDH activity in the culture supernatant was monitored at 3-h intervals after infection using a LDH cytotoxicity detection kit (TaKaRa BIO). In one experiment, cells were infected with H37Rv for 3 h, washed, and subsequently cultured with or without 1 mM EGTA, 40 μM MDL28170, and 100 μM calpain inhibitor IV for 21 h. The culture supernatant was collected, and LDH activity was measured. The maximum LDH release referred to the LDH value obtained from the supernatant of cells treated with 1% Triton X-100.

Intracellular Ca^{2+} level

Macrophages were plated at 1.25×10^5 cells $well^{-1}$ in 96-well black microplates (Invitrogen) and infected with *M. tuberculosis* H37Rv, ΔRD1, and ΔRD1::RD1 at a MOI of

5 for 3 h. The intracellular Ca^{2+} concentration was monitored at 3-h intervals for 21 h using a Fluo-4 NW Ca^{2+} assay kit (Invitrogen) according to the manufacturer's instructions.

Statistical analysis

Statistical analysis was performed using Student's *t*-test. A value of < 0.05 was considered to be statistically significant.

Results

The RD1 locus is indispensable for IL-1α secretion from *M. tuberculosis*-infected macrophages

Based on our investigation into the mechanism underlying the bacterial virulence factors that contribute to cytokine production by infected macrophages, we recently identified that the RD1 locus in the *M. tuberculosis* genome was critically involved in IL-1β and IL-18 secretions through the activation of caspase-1 (Kurenuma *et al.*, 2009). Furthermore, we also found that IL-1α secretion was highly dependent upon the RD1 locus. In this current study, therefore, we analyzed the mechanism underlying IL-1α secretion from *M. tuberculosis*-infected macrophages, specifically the role of the RD1 locus. IL-1α secretion by macrophages infected with the H37Rv strain, an RD1-deficient mutant (ΔRD1) strain, and an RD1-complemented (ΔRD1::RD1) strain was measured. We found that H37Rv, but not ΔRD1, induced a high level of IL-1α secretion from infected macrophages (Fig. 1a). Furthermore, complementation with the RD1 locus mostly restored the inability of ΔRD1 to induce IL-1α secretion (Fig. 1b). Interestingly, H37Rv and ΔRD1 induced comparable levels of IL-12/23p40 production. These results clearly demonstrated that RD1 is required for the secretion of IL-1α from infected macrophages, whereas it is dispensable for IL-12/23p40 production. To rule out the possibility that the difference between the induction of IL-1α in response to H37Rv and ΔRD1 infection was due to the efficacy of infection and replication of these bacteria strains, we measured their cfu numbers at 3 h and 24 h after infection. There was no significant difference in the number of bacteria recovered for these *M. tuberculosis* strains (Fig. 1d). Taken together, these results indicated that RD1 is indispensable for the induction of IL-1α secretion from H37Rv-infected macrophages.

RD1 is involved in the maturation and secretion of IL-1α, but does not participate in the induction of IL-1α transcription in H37Rv-infected macrophages

To analyze the mechanism by which RD1 facilitates IL-1α secretion from H37Rv-infected macrophages, we first determined the level of IL-1α mRNA expression after infection with H37Rv and ΔRD1 by real-time RT-PCR. A significant increase in IL-1α mRNA expression was detected in macrophages infected with H37Rv, and the levels were almost 20-fold higher than that observed in noninfected macrophages (Fig. 2a). Similarly, significantly high levels of IL-1α mRNA expression were also detected in macrophages infected with

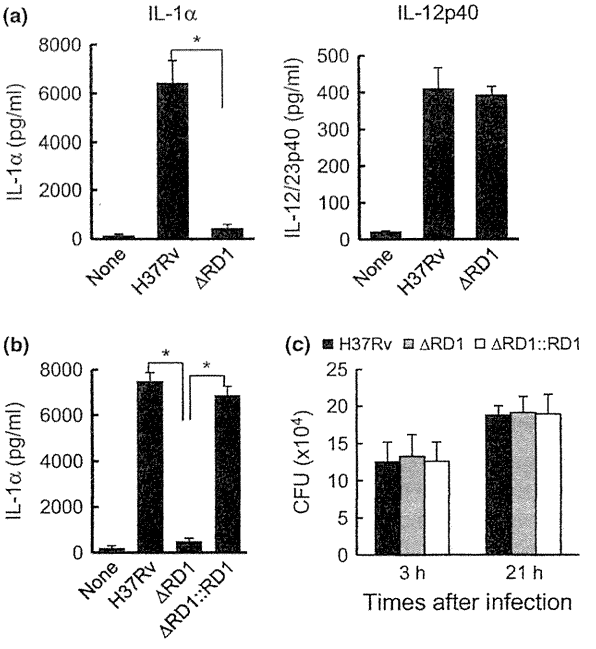

Fig. 1 RD1 contributes to IL-1α secretion from H37Rv-infected macrophages, but is dispensable for IL-12/23p40 production. Thioglycollate-induced peritoneal exudate macrophages were infected with H37Rv and ΔRD1 (a) or with H37Rv, ΔRD1, and ΔRD1::RD1 (b) at a MOI of 5 for 3 h. Cells were washed and then cultured for 21 h. The culture supernatant was collected, and the level of IL-1α and IL-12/23p40 was measured. (c) Macrophages were infected with H37Rv, ΔRD1, and ΔRD1::RD1 for 3 h. Cells were washed and then cultured for 21 h. Cells were lysed in 0.05% Triton X-100 solution after 3 h of infection and 21 h of cultivation. The cell lysate was inoculated on Middlebrook 7H10 agar plates, and the cfu number was counted 3 weeks later. Data represent the mean ± SD of triplicate assays and are representative of three independent experiments [$*P < 0.01$ (determined by Student's *t*-test)].

ΔRD1. We next compared the level of IL-1α synthesis and its secretion from macrophages infected with H37Rv and ΔRD1. IL-1α is synthesized as a 35-kDa precursor protein (pro-IL1α) that is subsequently converted into the mature IL-1α (17 kDa) and secreted into the extracellular space. To analyze the kinetics of IL-1α production in response to H37Rv and ΔRD1 infection, we quantified the total amount of IL-1α by determining the titer of mature IL-1α in the culture supernatant plus the titer of pro-IL-1α in the cell lysate. Consistent with the pattern of mRNA expression, IL-1α production was similarly observed as early as 3 h after infection with H37Rv and ΔRD1, and the levels gradually increased up to 21 h. There was no difference in the kinetics of IL-1α production after infection with H37Rv and ΔRD1 (Fig. 2b). On the other hand, IL-1α was detected only in the culture supernatant of H37Rv-infected macrophages, and ΔRD1 did not exert the ability to induce IL-1α secretion (Fig. 2c). Western blot analysis revealed similar levels of pro-IL1α synthesis in macrophages after infection with H37Rv and ΔRD1; however, significant IL-1α secretion was only observed in macrophages infected with H37Rv (Fig. 2d). These results indicated that while IL-1α transcription and pro-IL1α synthesis were induced

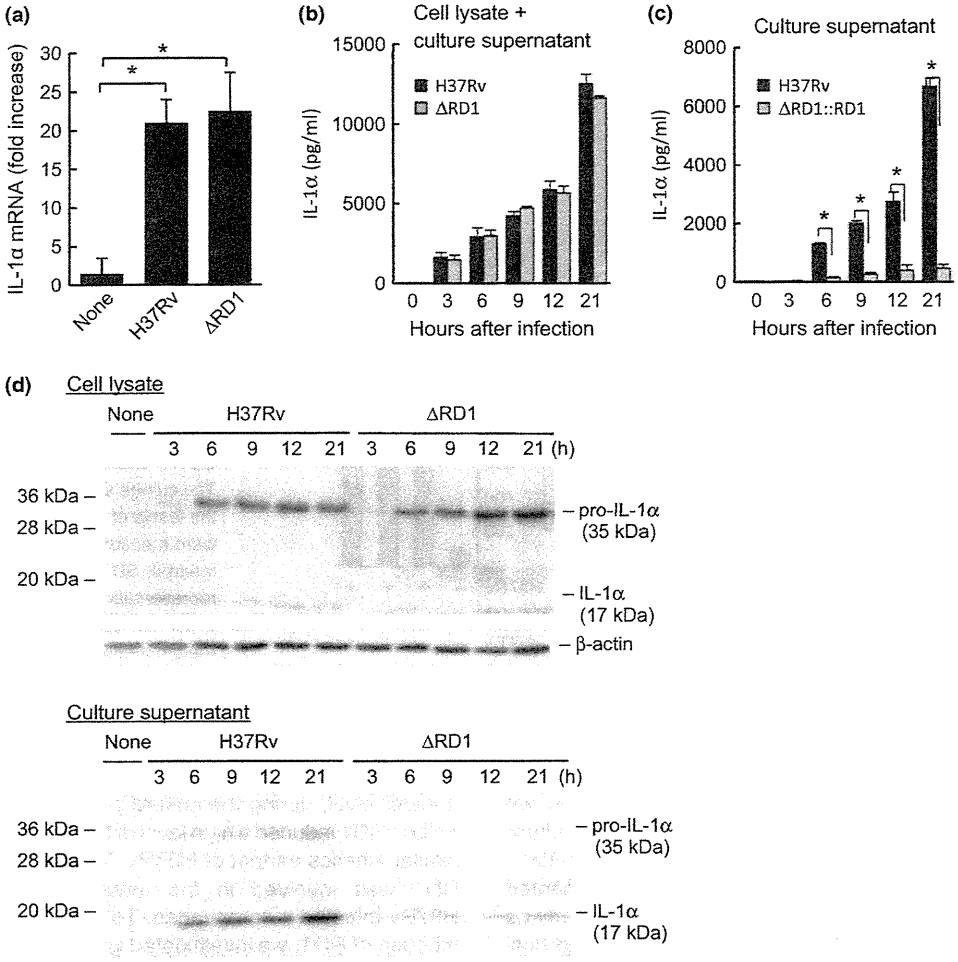

Fig. 2 RD1 is involved in IL-1α maturation and secretion, but not in IL-1α transcription or pro-IL-1α synthesis. (a) Macrophages were infected with H37Rv and ΔRD1 at a MOI of 5 for 3 h. Cells were washed and cultured for 3 h. Total RNA was extracted, and the level of IL-1α mRNA expression was analyzed by real-time RT-PCR. Data represent the mean ± SD of three independent experiments. (b, c) Macrophages were infected with H37Rv and ΔRD1 at a MOI of 5 for 3 h. Cells were washed and cultured for up to 21 h. The culture supernatant and the cell lysate were prepared at the indicated time after infection. The level of IL-1α production (b) was evaluated by a total of IL-1α concentration in the culture supernatant and the cell lysate. The level of secreted IL-1α (c) was determined by measuring the level of IL-1α in the culture supernatant. Data represent the mean ± SD of triplicate assays and are representative of three independent experiments. [$*P < 0.01$ (determined by Student's *t*-test)] (d) Macrophages were infected with H37Rv and ΔRD1 at a MOI of 5 for 3 h. Cells were washed and cultured for up to 24 h. The culture supernatant and the cell lysate were prepared at indicated times and subjected to SDS-PAGE. Mature IL-1α and pro-IL1α were detected by Western blotting. β-actin was detected to confirm that comparable amounts of cell lysates were applied to SDS-PAGE.

independently of RD1 in H37Rv-infected macrophages, the gene locus plays a role in the maturation and secretion of IL-1α.

Calpain is required for the secretion of IL-1α from H37Rv-infected macrophages

It has been shown that calpain, a Ca^{2+}-dependent cysteine protease, is activated by various stimuli and contributes to the maturation and secretion of IL-1α (Kobayashi *et al.*, 1990). To determine whether calpain is also involved in IL-1α secretion from H37Rv-infected macrophages, we investigated the effect of several calpain inhibitors on IL-1α secretion. As shown in Fig. 3, MDL28170 dramatically inhibited IL-1α secretion from H37Rv-infected macrophages in a dose-dependent manner. Furthermore, two other calpain inhibitors, calpain inhibitor IV and EST, also impaired IL-1α secretion. In addition, the Ca^{2+} chelators EGTA and BAPTA-AM markedly inhibited cytokine secretion. On the other hand, these reagents did not affect IL-12/23p40 secretion from H37Rv-infected macrophages. Taken together, these results suggested that calpain is involved in the secretion of IL-1α from H37Rv-infected macrophages. To further clarify the contribution of calpain to H37Rv-induced IL-1α secretion, we measured the activity of calpain in infected macrophages. It has been shown that α-fodrin, a

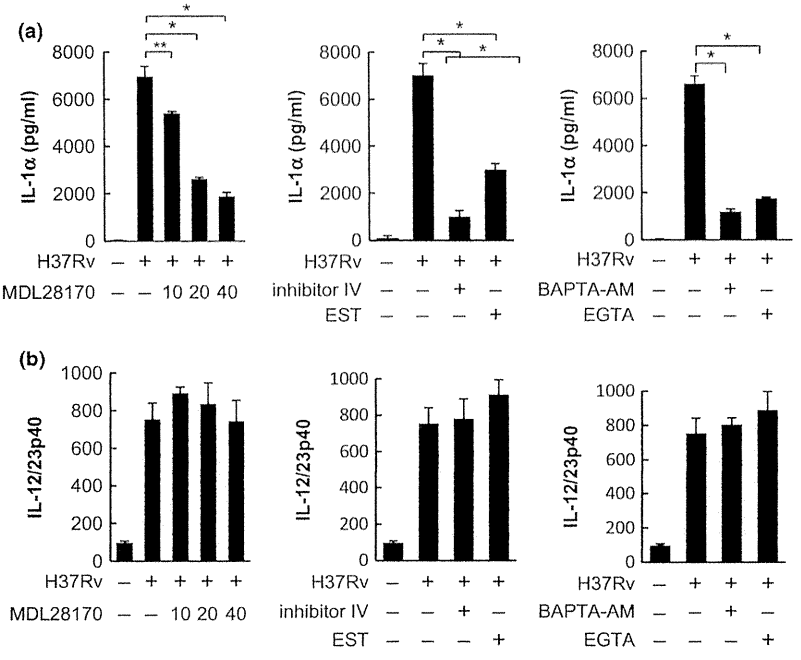

Fig. 3 *Calpain inhibitors and calcium chelators markedly inhibit IL-1α secretion from H37Rv-infected macrophages.* Macrophages were infected with H37Rv at a MOI of 5 for 3 h. Cells were washed and cultured for 3 h. Subsequently, cells were treated with 10–40 μM MDL28170, 100 μM calpain inhibitor IV, 100 μM EST, 1 mM EGTA, and 20 μM BAPTA-AM for 21 h. The culture supernatant was collected, and the levels of IL-1α (a) and IL-12/23p40 (b) were measured. Data represent the mean ± SD of triplicate assays and are representative of three independent experiments. [$*P < 0.01$. $**P < 0.05$ (determined by Student's *t*-test)].

240-kDa cytoskeletal protein, is an endogenous substrate of calpain, and the amount of the degraded fragment (145 kDa) released in the culture supernatant is indicative of calpain activity (Wang, 2000; Goll *et al.*, 2003). Thus, we analyzed the amount of fragmented α-fodrin in the culture supernatant after infection with H37Rv, ΔRD1, and ΔRD1::RD1. As shown in Fig. 4a, the amount of fragmented α-fodrin was detected in the culture supernatant as early as 6 h after infection with H37Rv and gradually increased until 24 h. However, ΔRD1 hardly induced the breakdown of α-fodrin. The kinetics of degraded product largely paralleled time-dependent IL-1α secretion. Moreover, H37Rv markedly decreased the amount of full-length α-fodrin in the cell lysate and increased the small fragment of α-fodrin in the culture supernatant (Fig. 4b). However, ΔRD1 infection induced a marginal level of α-fodrin fragmentation. On the other hand, significant levels of fragmented α-fodrin were observed in macrophages infected with ΔRD1::RD1. These results suggested that calpain was involved in IL-1α secretion from H37Rv-infected macrophages with RD1 playing a critical role in calpain activation.

RD1 is implicated in calpain activation and IL-1α secretion through the elevation of intracellular Ca^{2+} levels in H37Rv-infected macrophages

Calpain is a Ca^{2+}-dependent cysteine protease, and an increase in the cytosolic Ca^{2+} level plays a major role in calpain activation (Goll *et al.*, 2003). Therefore, we next analyzed the kinetics of cytosolic Ca^{2+} levels in macrophages infected with H37Rv, ΔRD1, and ΔRD1::RD1 using the Fluo-4 NW Ca^{2+} assay kit. H37Rv-infection markedly increased cytosolic Ca^{2+} levels as indicated by the high fluorescence intensity of Fluo-4. The fluorescence intensity was markedly enhanced 6 h after infection and maintained until 21 h (Fig. 5a). In contrast, ΔRD1 induced a weak fluorescence intensity compared with H37Rv, and it was sustained, albeit at a lower level, during the culture period. On the other hand, ΔRD1::RD1 induced a high level of fluorescence intensity with similar kinetics as that of H37Rv, Therefore suggesting that RD1 was involved in the induction of Ca^{2+} influx in H37Rv-infected macrophages. To further elucidate the contribution of RD1, we investigated whether A23187, a calcium ionophore, restored the inability of ΔRD1 to induce IL-1α secretion. As shown in Fig. 5b, ΔRD1 induced a low level of IL-1α secretion; however, treatment with A23187 significantly enhanced IL-1α secretion. These data suggested that RD1 contributes to the increase in cytosolic Ca^{2+} levels in infected macrophages, and the RD1-dependent Ca^{2+} influx leads to calpain activation and IL-1α secretion from infected macrophages.

Discussion

In this study, we examined the role of RD1 in IL-1α secretion from H37Rv-infected macrophages. Our results clearly showed that H37Rv infection induced a high level of IL-1α secretion, and RD1 was indispensable for the maturation and secretion of IL-1α; however, RD1 did not contribute to the induction of IL-1α transcription and pro-IL1α synthesis. Finally, RD1 was implicated in calpain activation through the increase of cytosolic Ca^{2+} levels.

Recent studies have shown that *M. tuberculosis* has TLR ligands, and the cytokine production by TLR2- and TLR4-deficient macrophages in response to *M. tuberculosis* is markedly decreased compared with that of WT macrophages (Means *et al.*, 2001). Therefore, it is highly likely that IL-1α production is mainly induced by a direct interaction of

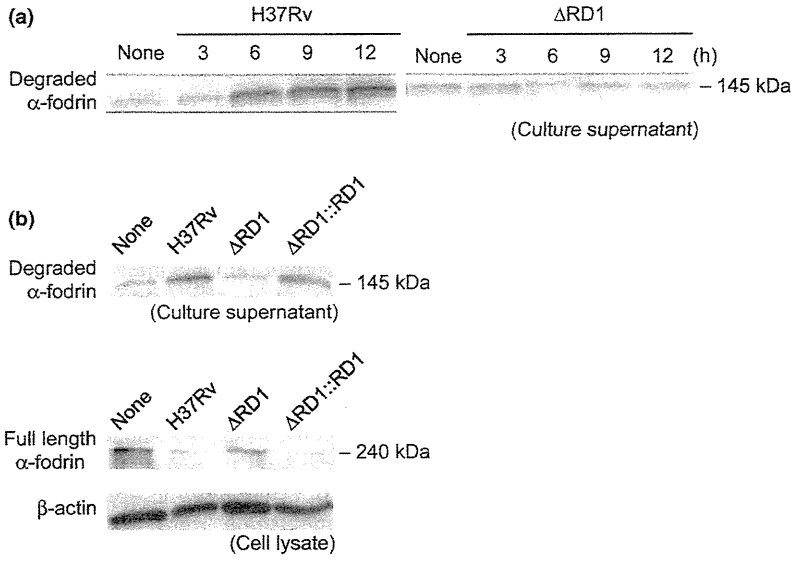

Fig. 4 *Mycobacterium tuberculosis* H37Rv but not ΔRD1 promotes fragmentation of α-fodrin in infected macrophages. (a) Macrophages were infected with H37Rv and ΔRD1 at a MOI of 5 for 3 h. Cells were washed and then cultured for the indicated periods. The culture supernatant was collected and subjected to SDS-PAGE. The amount of degraded fragment (145 kDa) of α-fodrin (an endogenous substrate of calpain) was monitored by Western blotting. (b) Macrophages were infected with H37Rv, ΔRD1, and ΔRD1::RD1 at a MOI of 5 for 3 h. Cells were washed and cultured for 21 h. The culture supernatant and the cell lysate were prepared concomitantly. They were subjected to SDS-PAGE, and the amount of full-length and fragmented α-fodrin was monitored. β-actin was detected to confirm that comparable amounts of cell lysates were applied to SDS-PAGE.

macrophages with *M. tuberculosis*. Furthermore, previous studies have shown that RD1 contributes to bacterial virulence, the generation of protective immunity (Pym *et al.*, 2003; Brodin *et al.*, 2006), granuloma formation (Volkman *et al.*, 2004), and necrosis induction (Hsu *et al.*, 2003; Junqueira-Kipnis *et al.*, 2006; Chen *et al.*, 2007; Kaku *et al.*, 2007). In addition, we have found that RD1 played a pivotal role in caspase-1 activation through facilitating K^+ efflux from the cytoplasm of infected macrophages (Kurenuma *et al.*, 2009). In this study, we demonstrated the active participation of RD1 in Ca^{2+} influx in infected macrophages. Based on these findings, we speculated that RD1 may provoke a perturbation of cytoplasmic membrane integrity, thus causing the transmembrane fluxes of calcium and potassium ions.

RD1 is located in the ESX-1 locus of the *M. tuberculosis* genome and includes genes encoding ESAT-6 and CFP-10 (Feltcher *et al.*, 2011). Both ESAT-6 and CFP-10, which belong to the WXG-100 superfamily, are secreted through the ESX-1 secretion system and form a protein complex (Brodin *et al.*, 2004b). Recent studies have shown that ESAT-6 exerts membrane lytic activity (Hsu *et al.*, 2003; de Jonge *et al.*, 2007) and influences a variety of signaling pathways (Yu & Xie, 2012). Therefore, it is probable that ESAT-6 may provoke the morphological alteration not only in the phagosomal membrane but also in the cytoplasmic membrane, resulting in the influx of intracellular Ca^{2+} level. Alternatively, recent reports have shown that the ESX-1 system may facilitate the diffusion of some bacterial products into the cytoplasm. Indeed, Mishra *et al.* have shown that ESAT-6 contributes to caspase-1 activation by facilitating the spread of immunostimulatory components into the cytoplasm (Mishra *et al.*, 2010). Wang *et al.* reported that ESAT-6 induced IL-1β secretion from human dendritic cells (Wang *et al.*, 2012). ESX-1 is required for the disruption of the phagosomal membrane and translocation of mycobacteria. Bacteria that have escaped from the phagosome subsequently secrete components through the ESX-5 system, which induce inflammasome activation, IL-1β secretion, and caspase-independent cell death (Abdallah *et al.*, 2011). Therefore, it is possible that RD1 may function in IL-1α production by inducing phagosomal membrane damage and the diffusion of some mycobacterial components that are required for Ca^{2+} influx, as well as calpain activation in the cytoplasm of infected macrophages. Alternatively, it has been shown that nucleotides including ATP and ADP induce calcium signaling in immune cells (Marteau *et al.*, 2004; Bendz *et al.*, 2008). Because wild-type *M. tuberculosis* causes necrosis of infected macrophages with a high frequency, therefore, it is probable that nucleotides released from necrotic cells may partly contribute to the intracellular Ca^{2+} mobilization. To clarify the precise mechanism of RD1 in IL-1α secretion, further studies are required to identify mycobacterial components that are directly responsible for the induction of Ca^{2+} influx.

RD1 is involved in the induction of necrotic cell death of infected macrophages by causing mitochondrial membrane damage and ATP depletion (Kaku *et al.*, 2007). Thus, we determined whether calpain participates in cell death of infected macrophages by measuring the release of LDH from cells infected with H37Rv in the presence of the calpain inhibitors MDL28170, inhibitor IV, and EGTA. The calpain

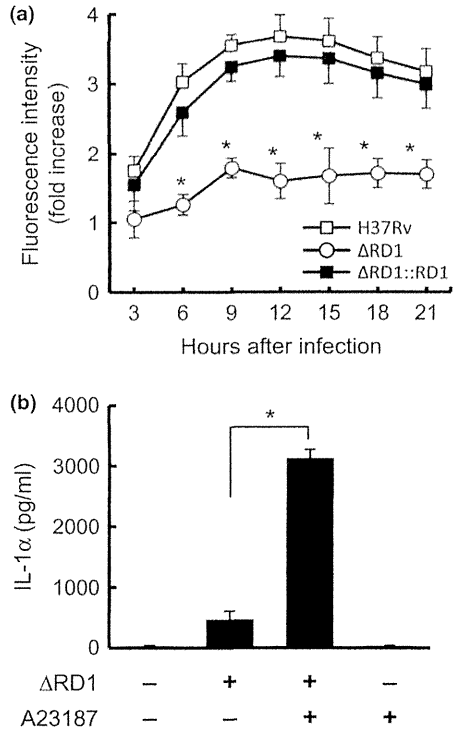

Fig. 5 RD1 contributes to the increase in cytosolic Ca^{2+} level in infected macrophages. (a) Macrophages were infected with H37Rv, ΔRD1, and ΔRD1::RD1 at a MOI of 5 for 3 h. Cells were washed and cultured for 3 h. The culture medium was removed, and cells were labeled with a dye-loading solution containing Fluo-4 NW. The fluorescence intensity was monitored for up to 21 h. (b) Macrophages were infected with ΔRD1 for 3 h. Cells were washed and cultured for 21 h in the presence of 10 μM A23187. The culture supernatant was collected, and the level of IL-1α secretion was measured. (−), no infection or no addition of A23187. Data represent the mean ± SD of triplicate assays and are representative of three independent experiments. [$*P < 0.01$ (determined by Student's *t*-test)].

inhibitors weakly, but significantly, prevented LDH release and largely abrogated IL-1α secretion (Fig. 2 and Supporting Information, Fig. S1). In this regard, previous studies reported that ESAT-6 was a potent activator of the NLRP3 inflammasome, and consequently, necrotic cell death of infected macrophages was triggered by ESAT-6-dependent NLRP3 inflammasome activation (Mishra *et al.*, 2010; Wong & Jacobs, 2011). Therefore, calpain was necessary to catalyze pro-IL-1α, but it likely only contributes to necrotic cell death of infected macrophages. On the other hand, EGTA also inhibited LDH release from infected macrophages, and its inhibitory activity was much stronger than those of the calpain inhibitors, suggesting that Ca^{2+} signaling was required for the cell death.

Pro-IL-1α, unlike pro-IL-1β, is thought to activate IL-1 receptor-dependent signal pathway in a similar manner as mature IL-1α. Therefore, the passive release of pro-IL-1α upon cell death serves as a danger signal and is capable of causing inflammation. Indeed, a sterile inflammatory response can be triggered by IL-1α released from dying cells (Chen *et al.*, 2007). In H37Rv-infected macrophages, a large portion of IL-1α secreted into the culture supernatant was converted to the mature form, while most IL-1α detected in the cell lysate remained in the proform, indicating an intracellular process that resulted in the preferentially secretion of mature IL-1α. Recent reports indicated that IL-1α secretion was closely related to IL-1β secretion. Gross *et al.* identified a distinct IL-1α secretion pathway that was dependent on inflammasome (Gross *et al.*, 2012). Fettelschoss *et al.* also showed that mature IL-1α secretion required activation of the inflammasome, and IL-1β served as a shuttle for IL-1α (Fettelschoss *et al.*, 2012). Furthermore, Zheng *et al.* recently showed that an intracellular form of IL-1 receptor 2 (IL-1R2) interacted with pro-IL-1α, preventing calpain cleavage. Caspase-1 cleaves IL-1R2, which allows cleavage of pro-IL-1α by calpain (Zheng *et al.*, 2013). Therefore, it appeared that caspase-1 and the inflammasome were not involved in the maturation of IL-1α, but the secretion of mature IL-1α was likely dependent on inflammasome, caspase-1, and IL-1β.

Calpains are intracellular Ca^{2+}-dependent cysteine proteases that are ubiquitously expressed, and more than 15 proteins belong to the calpain family (Croall & DeMartino, 1991). There is mounting evidence that indicates that calpains break down a wide variety of cytoskeletal, membrane-associated, and regulatory proteins and participate in signal transduction, apoptosis, and IL-1α secretion (Czuprynski & Brown, 1987; Carruth *et al.*, 1991; Chua *et al.*, 2000; Croall & Ersfeld, 2007; Dewamitta *et al.*, 2010; Sato *et al.*, 2011). In general, calpain activity is tightly regulated by the level of transcription, Ca^{2+} availability, autoproteolysis, phosphorylation, intracellular distribution, and endogenous inhibitors (Goll *et al.*, 2003). Our results showed that RD1 contributes to calpain activation through the increase in cytosolic Ca^{2+} levels in infected macrophages. Furthermore, IL-1α secretion by infected macrophages was significantly inhibited by MDL28170, which exerts broad-spectrum activities, and also by EST and calpain inhibitor IV, which preferentially inhibit calpain I and calpain II, respectively. The results suggested that calpain I and calpain II, two major calpains that are distinguished by the optimal Ca^{2+} concentration required for maximal activity, are possibly involved in the processing of IL-1α during *M. tuberculosis* infection. However, we cannot exclude the possibility that other calcium-dependent proteases may also contribute to the processing of IL-1α either alone or in combination with calpain.

Although it has long been believed that both pro- and mature IL-1α exert a similar activity through binding to IL-1 receptor, recent reports demonstrated that pro-IL-1α accumulated in the nucleus where it induced biological responses that were dependent upon the nuclear localization (Stevenson *et al.*, 1997; Cheng *et al.*, 2008; Luheshi *et al.*, 2009). Therefore, IL-1α can be regarded as a dual function cytokine, and it is unknown whether these two forms of IL-1α similarly contribute to the induction of host resistance to *M. tuberculosis*, as it has been shown that IL-1R-deficient mice are susceptible to *M. tuberculosis* infection and blocking of IL-1α increases their susceptibility.

Therefore, IL-1 signaling is definitely important for host resistance to *M. tuberculosis* (Fremond *et al.*, 2007; Guler *et al.*, 2011). Thus, it may be interesting to determine the role of pro- and mature IL-1α for the primary host resistance to *M. tuberculosis* infection.

In conclusion, our study clearly indicated that *M. tuberculosis* infection induced IL-1α mRNA expression and pro-IL-1α synthesis. These processes were independent of RD1. In contrast, RD1 was implicated in calpain activation, as well as the maturation and secretion of IL-1α through the elevation of intracellular Ca^{2+} level. These findings provide further insight into the interaction between the RD1 locus and the host cytokine response to *M. tuberculosis* infection.

Acknowledgements

This study was supported by a grant-in-aid for scientific research on priority areas from the Ministry of Education, Science, Culture and Sports of Japan, grants-in-aid for scientific research (B and C) and a grant-in-aid for young scientists (B) from the Japan Society for the Promotion of Science, and a grant-in-aid for research on emerging and reemerging infectious diseases from the Ministry of Health, Labor and Welfare of Japan.

Author's contribution

R.Y. and C.X. contributed equally to this work.

References

Abdallah AM, Gey van Pittius NC, Champion PA, Cox J, Luirink J, Vandenbroucke-Grauls CM, Appelmelk BJ & Bitter W (2007) Type VII secretion – mycobacteria show the way. *Nat Rev Microbiol* 5: 883–891.

Abdallah AM, Bestebroer J, Savage NDL *et al.* (2011) Mycobacterial secretion systems ESX-1 and ESX-5 play distinct roles in host cell death and inflammasome activation. *J Immunol* 187: 4744–4753.

Bendz H, Marincek B-C, Momburg F, Ellwart JW, Issels RD, Nelson PJ & Noessner E (2008) Calcium signaling in dendritic cells by human or mycobacterial Hsp70 is caused by contamination and is not required for Hsp70-mediated enhancement of cross-presentation. *J Biol Chem* 283: 26477–26483.

Brodin P, Majlessi L, Brosch R, Smith D, Bancroft G, Clark S, Williams A, Leclerc C & Cole ST (2004a) Enhanced protection against tuberculosis by vaccination with recombinant *Mycobacterium microti* vaccine that induces T cell immunity against region of difference 1 antigens. *J Infect Dis* 190: 115–122.

Brodin P, Rosenkrands I, Andersen P, Cole ST & Brosch R (2004b) ESAT-6 proteins: protective antigens and virulence factors? *Trends Microbiol* 12: 500–508.

Brodin P, Majlessi L, Marsollier L *et al.* (2006) Dissection of ESAT-6 system 1 of *Mycobacterium tuberculosis* and impact on immunogenicity and virulence. *Infect Immun* 74: 88–98.

Carruth LM, Demczuk S & Mizel SB (1991) Involvement of a calpain-like protease in the processing of the murine interleukin 1 alpha precursor. *J Biol Chem* 266: 12162–12167.

Chen CJ, Kono H, Golenbock D, Reed G, Akira S & Rock KL (2007) Identification of a key pathway for the sterile inflammatory response triggered by dying cells. *Nat Med* 13: 851–856.

Cheng W, Shivshankar P, Zhong Y, Chen D, Li Z & Zhong G (2008) Intracellular interleukin-1 alpha mediates interleukin-8 production induced by *Chlamydia trachomatis* infection via a mechanism independent of type I interleukin-1 receptor. *Infect Immun* 76: 942–951.

Chua BT, Guo K & Li P (2000) Direct cleavage by the calcium-activated protease calpain can lead to inactivation of caspases. *J Biol Chem* 275: 5131–5135.

Croall DE & DeMartino GN (1991) Calcium-activated neutral protease (calpain) system: structure, function, and regulation. *Physiol Rev* 71: 813–847.

Croall DE & Ersfeld K (2007) The calpains: modular designs and functional diversity. *Genome Biol* 8: 218.

Czuprynski CJ & Brown JF (1987) Purified human and recombinant murine IL-1α induced accumulation of inflammatory peritoneal neutrophils and mononuclear phagocytes: possible contributions to antibacterial resistance. *Microb Pathog* 3: 377–386.

de Jonge MI, Pehau-Arnaudet G, Fretz MM *et al.* (2007) ESAT-6 from *Mycobacterium tuberculosis* dissociates from its putative chaperone CFP-10 under acidic conditions and exhibits membrane-lysing activity. *J Bacteriol* 189: 6028–6034.

Dewamitta SR, Nomura T, Kawamura I *et al.* (2010) Listeriolysin O-dependent bacterial entry into the cytoplasm is required for calpain activation and interleukin-1 alpha secretion in macrophages infected with *Listeria monocytogenes*. *Infect Immun* 78: 1884–1894.

Dinarello CA (1996) Biologic basis for interleukin-1 in disease. *Blood* 87: 2095–2147.

Feltcher ME, Sullivan JT & Braunstein M (2011) Protein export systems of *Mycobacterium tuberculosis*: novel targents for drug development? *Future Microbiol* 5: 1581–1597.

Fettelschoss A, Kistowska M, LeibundGut-Landmann S *et al.* (2012) Inflammasome activation and IL-1β target IL-1α for secretion as opposed to surface expression. *P Natl Acad Sci USA* 108: 18055–18060.

Fremond CM, Togbe D, Doz E, Rose S, Vasseur V, Maillet I, Jacobs M, Ryffel B & Quesniaux VF (2007) IL-1 receptor-mediated signal is an essential component of MyD88-dependent innate response to *Mycobacterium tuberculosis* infection. *J Immunol* 179: 1178–1189.

Gao LY, Guo S, McLaughlin B, Morisaki H, Engel JN & Brown EJ (2004) A mycobacterial virulence gene cluster extending RD1 is required for cytolysis, bacterial spreading and ESAT-6 secretion. *Mol Microbiol* 53: 1677–1693.

Goll DE, Thompson VF, Li H, Wei W & Cong J (2003) The calpain system. *Physiol Rev* 83: 731–801.

Gross O, Yazdi AS, Thomas CJ, Masin M, Heinz LX, Guarda G, Quadroni M, Drexler SK & Tschopp J (2012) Inflammasome activators induce interleukin-1α secretion via distinct pathways with differential requirement for the protease function of caspase-1. *Immunity* 36: 388–400.

Grover A, Taylor J, Troudt J, Keyser A, Sommersted K, Schenkel A & Izzo AA (2008) Mycobacterial infection induces the secretion of high-mobility group box 1 protein. *Cell Microbiol* 10: 1390–1404.

Guinn KM, Hickey MJ, Mathur SK, Zakel KL, Grotzke JE, Lewinsohn DM, Smith S & Sherman DR (2004) Individual RD1-region genes are required for export of ESAT-6/CFP-10 and for virulence of *Mycobacterium tuberculosis*. *Mol Microbiol* 51: 359–370.

Guler R, Parihar SP, Spohn G, Johansen P, Brombacher F & Bachmann MF (2011) Blocking IL-1α but not IL-1β increases susceptibility to chronic *Mycobacterium tuberculosis* infection in mice. *Vaccine* 29: 1339–1346.

Hsu T, Hingley-Wilson SM, Chen B *et al.* (2003) The primary mechanism of attenuation of bacillus Calmette–Guerin is a loss of

secreted lytic function required for invasion of lung interstitial tissue. *P Natl Acad Sci USA* 100: 12420–12425.

Junqueira-Kipnis AP, Basaraba RJ, Gruppo V *et al.* (2006) Mycobacteria lacking the RD1 region do not induce necrosis in the lungs of mice lacking interferon-gamma. *Immunology* 119: 224–231.

Kaku T, Kawamura I, Uchiyama R, Kurenuma T & Mitsuyama M (2007) RD1 region in mycobacterial genome is involved in the induction of necrosis in infected RAW264 cell via mitochondrial membrane damage and ATP depletion. *FEMS Microbiol Lett* 274: 189–195.

Kobayashi Y, Yamomoto K, Saido T, Kawasaki H, Oppenheim JJ & Matsushima K (1990) Identification of calcium-activated neutral protease as a processing enzyme of human interleukin 1α. *P Natl Acad Sci USA* 87: 5548–5552.

Kurenuma T, Kawamura I, Hara H, Uchiyama R, Daim S, Dewamitta SR, Sakai S, Tsuchiya K, Nomura T & Mitsuyama M (2009) The RD1 locus in the *Mycobacterium tuberculosis* genome contributes to activation of caspase-1 induction of potassium ion efflux in infected macrophages. *Infect Immun* 77: 3992–4001.

Luheshi NM, Rothwell NJ & Brough D (2009) The dynamics and mechanisms of interleukin-1α and β nuclear import. *Traffic* 10: 16–25.

Mahairas GG, Sabo PJ, Hickey MJ, Singh DC & Stover CK (1996) Molecular analysis of genetic differences between *Mycobacterium bovis* BCG and virulent *M. bovis*. *J Bacteriol* 178: 1274–1282.

Majlessi L, Brodin P, Brosch R, Rojas MJ, Khun H, Huerre M, Cole ST & Leclerc C (2005) Influence of ESAT-6 secretion system 1 (RD1) of *Mycobacterium tuberculosis* on the interaction between mycobacteria and the host immune system. *J Immunol* 174: 3570–3579.

Marteau F, Communi D, Boeynaems J-M & Gonzalez NS (2004) Involvement of multiple P2Y receptors and signaling pathways in the action of adenine nucleotides diphosphates on human monocyte-derived dendritic cells. *J Leukoc Biol* 76: 796–803.

Mayer-Barber KD, Andrade BB, Barber DL, Hieny S, Feng CG, Caspar P, Oland S, Gordon S & Sher A (2001) Innate and adaptive interferons suppress IL-1α and IL-1β production by distinct pulmonary myeloid subsets during *Mycobacterium tuberculosis* infection. *Immunity* 35: 1023–1034.

Means TK, Jones BW, Schromm AB, Shurtleff BA, Smith JA, Keane J, Golenbock DT, Vogel SN & Fenton MJ (2001) Differential effects of a Toll-like receptor antagonist on *Mycobacterium tuberculosis*-induced macrophage responses. *J Immunol* 166: 4074–4082.

Mishra BB, Moura-Alves P, Sonawane A, Hacohen N, Griffiths G, Molta LF & Anes E (2010) *Mycobacterium tuberculosis* protein ESAT-6 is a potent activator of the NLRP3/ASC inflammasome. *Cell Microbiol* 12: 1046–1063.

O'Donnell MR, Padayatchi N, Kvasnovsky C, Werner L, Master I & Horsburgh CR Jr (2013) Treatment outcomes for extensively drug-resistant tuberculosis and HIV co-infection. *Emerg Infect Dis* 19: 416–424.

Patel NR, Zhu J, Tachado SD, Zhang J, Wan Z, Saukkonen J & Koziel H (2007) HIV Impairs TNF-α mediated macrophage apoptotic response to *Mycobacterium tuberculosis*. *J Immunol* 179: 6973–6980.

Pym AS, Brodin P, Brosch R, Huerre M & Cole ST (2002) Loss of RD1 contributed to the attenuation of the live tuberculosis vaccines *Mycobacterium bovis* BCG and *Mycobacterium microti*. *Mol Microbiol* 46: 709–717.

Pym AS, Brodin P, Majlessi L, Brosch R, Demangel C, Williams A, Griffiths KE, Marchal G, Leclerc C & Cole ST (2003) Recombinant BCG exporting ESAT-6 confers enhanced protection against tuberculosis. *Nat Med* 9: 533–539.

Sato K, Minegishi S, Takano J, Plattner F, Saito T, Asada A, Kawahara H, Iwata N, Saido TC & Hisanaga S (2011) Calpastatin, an endogenous calpain-inhibitor protein, regulates the cleavage of the Cdk5 activator p35 to p25. *J Neurochem* 117: 504–515.

Schaub FJ, Liles WC, Ferri N, Sayson K, Seifert RA & Bowen-Pope DF (2003) Fas and Fas-associated death domain protein regulate monocyte chemoattractant protein-1 expression by human smooth muscle cells through caspase- and calpain-dependent release of interleukin-1α. *Circ Res* 93: 515–522.

Sims JE & Smith DE (2010) The IL-1 family: regulators of immunity. *Nat Rev Immunol* 10: 89–102.

Stanley SA, Raghavan S, Hwang WW & Cox JS (2003) Acute infection and macrophage subversion by *Mycobacterium tuberculosis* require a specialized secretion system. *P Natl Acad Sci USA* 100: 13001–13006.

Stanley SA, Johndrow JE, Manzanillo P & Cox JS (2007) The Type I IFN response to infection with *Mycobacterium tuberculosis* requires ESX-1-mediated secretion and contributes to pathogenesis. *J Immunol* 178: 3143–3152.

Stevenson FT, Turck J, Locksley RM & Lovett DH (1997) The N-terminal propiece of interleukin 1 alpha is a transforming nuclear oncoprotein. *P Natl Acad Sci USA* 94: 508–513.

Volkman H, Clay H, Beery D, Chang J, Sherman D & Ramakrishnan L (2004) Tuberculous granuloma formation is enhanced by a mycobacterium virulence determinant. *PLoS Biol* 2: e367.

Wang KK (2000) Calpain and caspase: can you tell the difference? *Trends Neurosci* 23: 20–26.

Wang X, Barnes PF, Huang F, Alvarez IB, Neuenschwander PF, Sherman DR & Samten B (2012) Early secreted antigenic target of 6-kDa protein of *Mycobacterium tuberculosis* primes dendritic cells to stimulate Th17 and inhibit Th1 immune responses. *J Immunol* 189: 3092–3103.

Wong K-W & Jacobs WR Jr (2011) Critical role for NLRP3 in necrotic death triggered by *Mycobacterium tuberculosis*. *Cell Microbiol* 13: 1371–1384.

World Health Organization (2012) Global tuberculosis report 2012. http://www.who.int/tb/publications/global_report/en/

Yu X & Xie J (2012) Roles and underlying mechanisms of ESAT-6 in the context of *Mycobacterium tuberculosis*-host interaction from a systems biology perspective. *Cell Signal* 24: 1841–1846.

Zheng Y, Humphry M, Maguire JJ, Bennett MR & Clarke MCH (2013) Intracellular interleukin-1 receptor 2 binding prevents cleavage and activity of interleukin-1α, controlling necrosis-induced sterile inflammation. *Immunity* 38: 285–295.

Supporting Information

Additional Supporting Information may be found in the online version of this article:

Fig. S1. RD1 contribute to LDH release from H37Rv-infected macrophages independently of calpain activation.

genome Journals.ASM.org

Whole-Genome Sequence of *Mycobacterium kyorinense*

Kouki Ohtsuka,[a] Hiroaki Ohnishi,[a] Eriko Nozaki,[a] Jesus Pais Ramos,[b] Enrico Tortoli,[c] Shota Yonetani,[a] Satsuki Matsushima,[a] Yoshitaka Tateishi,[d] Sohkichi Matsumoto,[d] Takashi Watanabe[a]

Department of Laboratory Medicine, Kyorin University School of Medicine, Tokyo, Japan[a]; National Reference Laboratory for Tuberculosis, Centro de Referência Professor Hélio Fraga, Escola Nacional de Saúde Pública, Fiocruz, Rio de Janeiro, Brazil[b]; Emerging Bacterial Pathogens Unit, San Raffaele Scientific Institute, Milan, Italy[c]; Department of Bacteriology, Niigata University Graduate School of Medicine, Niigata, Japan[d]

We report here the first draft genome sequence of *Mycobacterium kyorinense*, which was described in 2009 and exhibits significant pathogenicity to humans.

Received 9 September 2014 **Accepted** 10 September 2014 **Published** 16 October 2014

Citation Ohtsuka K, Ohnishi H, Nozaki E, Pais Ramos J, Tortoli E, Yonetani S, Matsushima S, Tateishi Y, Matsumoto S, Watanabe T. 2014. Whole-genome sequence of *Mycobacterium kyorinense*. Genome Announc. 2(5):e01062-14. doi:10.1128/genomeA.01062-14.

Address correspondence to Hiroaki Ohnishi, onishi@ks.kyorin-u.ac.jp.

ycobacterium kyorinense is a slow-growing mycobacterium that was first described in 2009 (1). *M. kyorinense* is closely related to *M. celatum*, *M. branderi*, and *M. fragae*, and exhibits significant pathogenicity for humans, causing pneumonia, lymphadenitis, and arthritis (2–4). Antimicrobial susceptibility tests demonstrated that *M. kyorinense* is generally resistant to rifampin, isoniazid, and ethambutol (4). Further investigation is needed to clarify the genomics, biology, epidemiology, and pathogenicity of this species.

We sequenced the genomic DNA of the *M. kyorinense* type strain KUM060204^T on an Ion PGM system (Life Technologies) and assembled the reads using CLC Genomics Workbench 7.0. A total of 4,133,490 reads were generated, with an average read length of 203 bp, yielding a total sequence of 837,657,777 bp.

The assembled sequences of KUM060204^T comprised 453 contigs, with a combined length of 5,302,980 bp, with a G+C ratio of 66.9%. The average cover depth was 50×, the N_{50} contig size was 53,523, the average contig was 11,706 bp long, and the longest contig was 137,319 bp.

Genome annotation was performed using the RAST prokaryotic genome annotation server (http://www.nmpdr.org/FIG/wiki/view.cgi/Main/RAST). RAST predicted 5,405 putative open reading frames, including 5,351 coding sequences and 54 RNAs (46 tRNAs and 8 rRNAs). RAST functional analysis of the predicted protein-coding genes showed 78 genes involved in cell walls and capsules, 64 in membrane transport, 206 in protein metabolism, 93 in DNA metabolism, 141 in virulence and defense, 135 in respiration, 331 in fatty acids, lipids, and isoprenoids, 395 in cofactors, vitamins, prosthetic groups, and pigments, and 356 in amino acids and derivatives.

To explore the molecular mechanism underlying the resistance of *M. kyorinense* to anti-tuberculosis drugs, we selected several genes known to be responsible for resistance to rifampin (*rpoB*), ethambutol (*embB*), and isoniazid (*inhA*, *katG*, and *ahpC*). The sequences of these genes in *M. kyorinense* were compared with those in *M. tuberculosis* H37Rv to clarify whether they contain specific mutations associated with resistance to anti-tuberculosis drugs in *M. tuberculosis*. Analysis of the *rpoB* gene confirmed our previous finding that KUM060204^T harbors a Ser531Asp amino acid substitution, the most frequent mutation in rifampin-resistant *M. tuberculosis* (4, 5). In contrast, we did not detect a substitution at Met306 of *embB*, the major mutation in ethambutol-resistant *M. tuberculosis* (6). Nor did we find a Ser315Thr substitution of *katG*, a mutation in the regulatory region (nucleotides [nt] −48, −51, −54, −81, and −88) of *ahpC*, a Ser94Ala substitution in the *inhA* gene or a mutation in the regulatory region (nt −15 and −17) of *inhA*, which are common mutations in isoniazid-resistant *M. tuberculosis* (6). These results suggested that the mechanism underlying drug resistance in *M. kyorinense* is significantly different from that in *M. tuberculosis*.

In conclusion, we report the genome sequence of KUM060204^T which to the best of our knowledge is the first genome sequence of the species *M. kyorinense*.

Nucleotide sequence accession numbers. The whole genome sequence of KUM060204^T has been deposited in DDBJ/EMBL/GenBank under the accession numbers BBKA01000001 to BBKA01000453.

ACKNOWLEDGMENTS

This work was supported by a grant from the Ministry of Education, Culture, Sports, Science, and Technology of Japan (23590688).

REFERENCES

1. Okazaki M, Ohkusu K, Hata H, Ohnishi H, Sugahara K, Kawamura C, Fujiwara N, Matsumoto S, Nishiuchi Y, Toyoda K, Saito H, Yonetani S, Fukugawa Y, Yamamoto M, Wada H, Sejimo A, Ebina A, Goto H, Ezaki T, Watanabe T. 2009. *Mycobacterium kyorinense* sp. nov., a novel, slow-growing species, related to *Mycobacterium celatum*, isolated from human clinical specimens. Int. J. Syst. Evol. Microbiol. 59:1336–1341. http://dx.doi.org/10.1099/ijs.0.000760-0.
2. Ramos JP, Campos CE, Caldas PC, Ferreira NV, da Silva MV, Redner P, Campelo CL, Vale SF, Barroso EC, Medeiros RF, Montes FC, Galvão TC, Tortoli E. 2013. *Mycobacterium fragae* sp. nov., a non-chromogenic species isolated from human respiratory specimens. Int. J. Syst. Evol. Microbiol. 63:2583–2587. http://dx.doi.org/10.1099/ijs.0.046862-0.
3. Campos CE, Caldas PC, Ohnishi H, Watanabe T, Ohtsuka K, Matsushima S, Ferreira NV, da Silva MV, Redner P, de Carvalho LD, Medeiros RF, Abbud Filho JA, Montes FC, Galvão TC, Ramos JP. 2012. First

isolation of *Mycobacterium kyorinense* from clinical specimens in Brazil. J. Clin. Microbiol. 50:2477–2478. http://dx.doi.org/10.1128/JCM.00023-12.
4. **Ohnishi H, Yonetani S, Matsushima S, Wada H, Takeshita K, Kuramochi D, Caldas PC, Campos CE, da Costa BP, Ramos JP, Mikura S, Narisawa E, Fujita A, Funayama Y, Kobashi Y, Sakakibara Y, Ishiyama Y, Takakura S, Goto H, Watanabe T.** 2013. *Mycobacterium kyorinense* infection. Emerg. Infect. Dis. 19: 508–510. http://dx.doi.org/10.3201/eid1903.120591.
5. **Telenti A, Imboden P, Marchesi F, Lowrie D, Cole S, Colston MJ, Matter L, Schopfer K, Bodmer T.** 1993. Detection of rifampicin-resistance mutations in *Mycobacterium tuberculosis*. Lancet 341:647–650. http://dx.doi.org/10.1016/0140-6736(93)90417-F.
6. **Zhang Y, Telenti Y.** 2000. Genetics of drug resistance in *Mycobacterium tuberculosis*, p 235–254. *In* Hatfull GF, Jacobs WR (ed), Molecular genetics of *Mycobacteria*. ASM Press, Washington, D.C.

Direct detection of *Mycobacterium avium* in environmental water and scale samples by loop-mediated isothermal amplification

Yukiko Nishiuchi, Aki Tamaru, Yasuhiko Suzuki, Seigo Kitada, Ryoji Maekura, Yoshitaka Tateishi, Mamiko Niki, Hisashi Ogura and Sohkichi Matsumoto

ABSTRACT

We previously demonstrated the colonization of *Mycobacterium avium* complex in bathrooms by the conventional culture method. In the present study, we aimed to directly detect *M. avium* organisms in the environment using loop-mediated isothermal amplification (LAMP), and to demonstrate the efficacy of LAMP by comparing the results with those obtained by culture. Our data showed that LAMP analysis has detection limits of 100 fg DNA/reaction for *M. avium*. Using an FTA® elute card, DNA templates were extracted from environmental samples from bathrooms in the residences of 29 patients with pulmonary *M. avium* disease. Of the 162 environmental samples examined, 143 (88%) showed identical results by both methods; 20 (12%) and 123 (76%) samples were positive and negative, respectively, for *M. avium*. Of the remaining 19 samples (12%), seven (5%) and 12 (7%) samples were positive by the LAMP and culture methods, respectively. All samples that contained over 20 colony forming units/primary isolation plate, as measured by the culture method, were also positive by the LAMP method. Our data demonstrate that the combination of the FTA elute card and LAMP can facilitate prompt detection of *M. avium* in the environment.

Key words | bathroom, direct detection, FTA elute card, loop-mediated isothermal amplification (LAMP), *Mycobacterium avium*

Yukiko Nishiuchi (corresponding author)
Toneyama Institute for Tuberculosis Research,
Osaka City University Medical School,
5-1-1 Toneyama, Toyonaka, Osaka 560-8552,
Japan
E-mail: *nishiuchi@med.osaka-cu.ac.jp*

Aki Tamaru
Department of Infectious Diseases,
The Osaka Prefectural Institute of Public Health,
1-3-69 Nakamichi, Higashinari-ku, Osaka 537-0025,
Japan

Yasuhiko Suzuki
Research Center for Zoonosis Control,
Hokkaido University, North 20, West 10 Kita-ku,
Sapporo, Hokkaido 001-0020,
Japan

Seigo Kitada
Ryoji Maekura
Yoshitaka Tateishi
National Hospital Organization Toneyama National Hospital, 5-1-1 Toneyama,
Toyonaka, Osaka 560-8552,
Japan

Yoshitaka Tateishi
Mamiko Niki
Sohkichi Matsumoto
Department of Bacteriology,
Osaka City University Graduate School of Medicine,
1-4-3 Asahi-machi, Abeno-ku, Osaka 545-8585,
Japan

Hisashi Ogura
Department of Virology,
Osaka City University Graduate School of Medicine,
1-4-3 Asahi-machi, Abeno-ku, Osaka 545-8585,
Japan

INTRODUCTION

The incidence of *Mycobacterium avium* complex (MAC) infection is gradually increasing all over the world, especially in developed countries (Falkinham 1996; Field *et al.* 2004; Griffith *et al.* 2007). MAC organisms inhabit the environment and are transferred to susceptible humans or farm animals, leading to infection and disease (Falkinham 2002; Field *et al.* 2004; Angenent *et al.* 2005). *M. avium* and other nontuberculous mycobacteria are widely distributed in natural and artificial environmental habitats, including natural water bodies, drinking water distribution systems, hot tubs, forest soils, peats, and potting soils (Falkinham 2009). We previously reported that MAC was frequently detected in

doi: 10.2166/wh.2013.007

samples from bathrooms in the residences of patients with pulmonary MAC disease, suggesting that the bathroom is the possible source of infection (Nishiuchi *et al.* 2007, 2009). Although MAC colonization in the human environment was polyclonal and displayed genetic diversity, some genotypes were identical or similar to the clinical isolates obtained from the corresponding patients (Nishiuchi *et al.* 2007, 2009). Moreover, the characteristics of MAC disease, such as multiple infections with genetically different strains (Wallace *et al.* 1998, 2002) and frequent relapse or reinfection (Kobashi & Matsushima 2003), could be attributable to the presence of a reservoir for MAC in the environment immediately surrounding the patients. It is important to break this cycle of infection by removing the infection source; identification of the source in the environment is thus the initial important step for controlling the disease.

In previous investigations, we isolated *M. avium* organisms by conventional culture. Although this method is basic and essential for the assessment of genetic diversity and drug susceptibility, the procedure is time consuming; it takes 3 weeks to obtain primary isolates and another 2 weeks to obtain pure cultures, followed by polymerase chain reaction (PCR) analysis for species identification (Nishiuchi *et al.* 2007, 2009). Thus, at least 5 weeks are usually required to detect *M. avium* organisms, underscoring the need for an alternative, rapid, and accurate method of *M. avium* detection in environmental specimens, which would in turn facilitate accelerated diagnosis. Nucleic acid amplification (NAA) tests are commonly used in hospitals to directly detect *Mycobacterium tuberculosis* and *M. avium* in clinical specimens because they require less time than culture. Several recent systematic investigations have confirmed the high specificity and sensitivity of NAA tests (Ichiyama *et al.* 1996; Soini & Musser 2001; Huggett *et al.* 2003; Park *et al.* 2006). A novel NAA method, termed loop-mediated isothermal amplification (LAMP), is commonly used to detect viruses, parasitic protozoans, and bacteria including *M. tuberculosis* complex (Iwamoto *et al.* 2003; Boehme *et al.* 2007; Pandey *et al.* 2008), *M. avium* (Iwamoto *et al.* 2003), *M. avium* subsp. *paratuberculosis* (Enosawa *et al.* 2003), *M. intracellulare* (Iwamoto *et al.* 2003), *M. kansasii* (Mukai *et al.* 2006) and *M. gastri* (Mukai *et al.* 2006). The LAMP method has been applied to detect mycobacteria in clinical samples (Iwamoto *et al.* 2003; Boehme *et al.* 2007; Pandey *et al.* 2008), but it has not been tested for environmental samples. In the present study, environmental samples obtained previously (Nishiuchi *et al.* 2009) were subjected to LAMP analysis for the direct detection of *M. avium* using novel primer sets targeting the *M. avium* 16S rRNA gene. The results were compared with those obtained previously by culture (Nishiuchi *et al.* 2009). We also employed FTA® elute cards for genomic DNA extraction; these cards allowed very easy recovery of DNA templates from the environmental samples without resorting to the use of any harmful reagent.

METHODS

Design of LAMP primers

Using conserved sequences of the 16S rRNA gene as a target, two inner primers, namely the forward inner primer (FIP) and backward inner primers (BIP), two outer primers (F3 and B3), and two loop primers (FL and BL) for *M. avium* were designed using PrimerExplorer V3 software (https://primerexplorer.jp; Eiken Chemical Co. Ltd, Tokyo, Japan). The primer sequences and other details are listed in Table 1.

LAMP reaction

LAMP was performed in 50 μl reaction volumes containing 4 μl of the extracted DNA template, 20 μmol l^{-1} each of FIP and BIP, 25 μmol l^{-1} each of F3 and B3, 30 μmol l^{-1} each of FL and BL, 1.4 mmol l^{-1} deoxynucleoside triphosphate mix, 0.8 mol l^{-1} betaine (Sigma-Aldrich, St Louis, MO, USA), 20 mmol l^{-1} Tris-HCl (pH 8.8), 10 mmol l^{-1} KCl, 10 mmol l^{-1} $(NH_4)_2SO_4$, 8 mmol l^{-1} $MgSO_4$, and 6.4 U of *Bst* DNA polymerase (large fragment; New England Biolabs Inc., Beverly, MA, USA). The mixture was incubated at 64 °C for 60 min in a Loopamp® real-time turbidimeter (LA-200; Teramecs Co., Kyoto, Japan) and then heated to 80 °C for 2 min to terminate the reaction.

Analysis of LAMP products

The LAMP reaction causes turbidity in the reaction tube, which is proportional to the amount of amplified DNA. The reaction was considered positive when a turbidity of ≥0.1 was observed